Food Chemistry 499 (2026) 147361

Contents lists available at ScienceDirect

Food Chemistry

journal homepage: www.elsevier.com/locate/foodchem

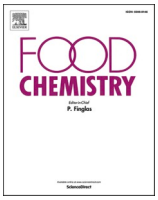

# Systematic identification of novel glycosidic aromatic precursors in winemaking grapes via preparative LC fractionation, target GC and non-targeted UHPLC-MS analysis

Belén González-Martínez, Elayma Sánchez-Acevedo, Arancha de-la-Fuente-Blanco, Ignacio Ontañón, Ricardo Lopez, Vicente Ferreira *

*Laboratorio de Análisis del Aroma y Enología (LAAE), Department of Analytical Chemistry, Universidad de Zaragoza, Instituto Agroalimentario de Aragón (IA2) (UNIZAR-CITA), Associate unit to Instituto de las Ciencias de la Vid y el Vino (ICVV) (UR-CSIC-GR), c/ Pedro Cerbuna 12, 50009 Zaragoza, Spain*

ARTICLE INFO

*Keywords:*
Aromatic precursors
Acid hydrolysis
Grape aroma
Phenolic aromatic fraction
Glycosides

ABSTRACT

Grapes used in winemaking contain non-volatile precursors that, through chemical reactions and rearrangements, release key aromatic compounds essential to wine aroma. This study aims to identify aroma precursors in extracts from 'Garnacha' grapes combining sequential C18, semi-preparative chromatographies (size exclusion + normal phase), target SPME-GC–MS analysis of the hydrolysed fractions and untargeted UHPLC-MS of the original fractions. Ninety-nine fractions were obtained, 92 of which released aroma upon hydrolysis. Targeted aroma compounds (terpenes, norisoprenoids, volatile phenols, vanillins and ethyl cinnamates) were detected in the hydrolysates of 55 fractions. Identification of precursors was based on: a) exact molecular mass, b) MS/MS spectrum, and c) correlation between the precursor and aroma signals in UHPLC-MS and GC–MS in the original and hydrolysed fractions, respectively. Overall, 185 precursors were identified, 98 for the first time, including 94 disaccharides, 57 trisaccharides and 34 monosaccharides from: terpenes (83), volatile phenols (30), cinnamic acid derivatives (22), norisoprenoids (21), vanillins (19), ethyl leucate (6) and furaneol (4). This work represents a significant advancement in the evaluation of the potential aromatic quality of winemaking grapes using UHPLC-MS.

## 1. Introduction

Winemaking grapes are aromatically neutral, and their subtle aroma and flavour are due to the presence of small amounts of aromatic compounds such as $\beta$-damascenone, furaneol, certain terpenols, benzenoids, and volatile phenols, among others (Ferreira & López, 2019). In addition to the presence of these molecules in their free form, grapes contain a complex series of aromatic precursors (Baumes, 2009). These are non-volatile molecules capable of generating a volatile molecule with aromatic properties (odourant) through the simple cleavage of a chemical bond, often followed (or preceded) by other spontaneous molecular rearrangement processes. These aromatic compounds, present in the form of non-volatile precursors, play an essential role in wine quality (Salinas et al., 2012), as they represent an important source of aroma that manifests during wine fermentation and aging through enzymatic and/or acid hydrolysis (Parker et al., 2018).

Among the aromatic precursors, the most abundant are glycosidic precursors (Liu et al., 2017), although there are other types of minor precursors formed by aromatic compounds bound to cystine or glutathione. Glycosidic precursors consist of an aglycone linked by an *O*-glycosidic linkage to one or more sugar molecules (glycone). Glycosylation increases the water solubility and reduces the reactivity of aromatic compounds, which in turn facilitates their transport, accumulation, storage, and reduces the toxicity of these volatile compounds to plants (Hjelmeland & Ebeler, 2015).

In general, the aglycones present in grapes include terpenoids, norisoprenoids, aliphatic alcohols, volatile phenols, and benzenoids (Caffrey et al., 2020). On the other hand, the glycans identified so far are mainly disaccharides, followed by monosaccharides and trisaccharides in smaller proportions, the latter being less abundant than the other two types (Caffrey et al., 2020; D'Ambrosio et al., 2013; Schievano et al., 2013). Among these glycans, $\beta$-*D*-glucopyranoside has been described as

* Corresponding author.
*E-mail addresses:* b.gonzalez@unizar.es (B. González-Martínez), esanchezacevedo@unizar.es (E. Sánchez-Acevedo), arandlfb@unizar.es (A. de-la-Fuente-Blanco), ionta@unizar.es (I. Ontañón), riclopez@unizar.es (R. Lopez), vferre@unizar.es (V. Ferreira).

https://doi.org/10.1016/j.foodchem.2025.147361
Received 30 July 2025; Received in revised form 21 November 2025; Accepted 29 November 2025
Available online 1 December 2025
0308-8146/© 2025 The Authors. Published by Elsevier Ltd. This is an open access article under the CC BY-NC-ND license (http://creativecommons.org/licenses/by-nc-nd/4.0/).

a monosaccharide, while *α-L*-rhamnopyranosyl-*β-D*-glucopyranoside, *α-L*-arabinofuranosyl-*β-D*-glucopyranoside, and *α-L*-apiofuranosyl-*β-D*-glucopyranoside have been identified as disaccharides (Hjelmeland & Ebeler, 2015). In addition, various trisaccharides have been identified, including hexose-pentose-hexose, hexose-hexose-hexose, and pentose-pentose-hexose (Hjelmeland et al., 2015).

The first methodologies used to study the glycosidic precursors present in grapes, which are still in use today, are based on the release of the aglycone through acid or enzymatic hydrolysis and its subsequent identification and quantification by gas chromatography coupled with mass spectrometry detection (GC–MS) (Gunata et al., 1990; Loscos et al., 2009; Wang et al., 2020). However, these strategies have several limitations, including hydrolysis time, efficiency, and potential structural modifications.

Enzymatic hydrolysis generally does not require long incubation times, but its efficiency is strongly influenced by the enzymes used (*endo-* or *exo*-glucosidases), the specific aglycone, and inhibitory factors commonly present in grapes and wine, such as high ethanol content, low pH, and/or elevated glucose concentrations (Gunata et al., 1990; Sarry & Günata, 2004). Although enzymatic hydrolysis typically causes fewer structural rearrangements of aglycones than acid hydrolysis (Gunata et al., 1985), it may not effectively release certain aglycones and could even result in the identification of artefactual aglycones produced through enzymatic oxidation (Hampel et al., 2014). Furthermore, some relevant odorants with known precursors lack the hydroxyl groups required for glycosylation, meaning that the aglycone is not the odorant, but a hydroxylated precursor whose structure may not be easily related to the odorant.

On the other hand, although acid hydrolysis is more economical than enzymatic hydrolysis and is not inhibited by high glucose levels (Liu et al., 2017), it may cause structural modifications and rearrangements of the aglycones (Mateo & Jiménez, 2000). Consequently, the identified compounds may not correspond to the native aglycone structures (Skouroumounis & Sefton, 2000). Nevertheless, in terms of the overall aroma potential, acid hydrolysis provides a more accurate representation of grape and wine aroma than enzymatic hydrolysis, as it allows for hydrolysis and molecular rearrangement processes that occur naturally during winemaking (Ferreira & López, 2019).

For all these reasons, although these strategies can be a very useful tool for evaluating the overall aromatic potential of winemaking grapes, they are not useful for elucidating the structures of glycosidic precursors. It should be noted that the information provided by these methods is limited, as they are indirect methods (based on the analysis of the resulting aromatic molecule) and therefore do not allow the determination of the exact structure of the aromatic precursor.

The recent advancement of ultra-high performance liquid chromatography coupled with mass spectrometry detectors (UHPLC-MS) has enabled the direct determination of glycosidic precursors. These developments have significantly improved both the chromatographic separation capability and detector resolution, allowing for direct determination without the risk of rearrangements in aglycone structures (Wei et al., 2021). The information provided by this strategy is highly relevant for elucidating the metabolic processes involved in the synthesis and accumulation of aromatic precursors.

However, the analysis is not without difficulties for several reasons:

- There are no commercial standards, which makes it difficult to unambiguously identify the molecules (Caffrey et al., 2020; Hjelmeland et al., 2015).
- The number of possible aromatic precursors for some relevant molecules, such as linalool or *β*-damascenone, can be high. In both cases, the precursors can be glycosides, whose glycone can consist of one, two, or three monosaccharide units of different types, and in both cases, the aglycone part can consist of several slightly different chemical structures that, after spontaneous processes, end up forming the aromatic molecule (Ferreira & López, 2019). In the case of linalool, there may also be non-glycosylated precursors (polyols).
- In addition to various glycosides and polyols, the family of precursors includes other chemical structures. In particular, polyfunctional mercaptans have precursors such as various cysteine conjugates (linked or not to other amino acids). The main precursor of dimethyl sulphide is *S*-methylmethionine (Cordente et al., 2015; Subileau et al., 2008a, 2008b). For lactones, the precursors could be the corresponding opened hydroxy acids (Ferreira & López, 2019), glycosylated or in free form. In the case of molecules with aldehyde or diketone groups, the precursors could be the corresponding adducts of molecules with $SO_2$ (hydroxyalkylsulfonates). The chemical diversity is therefore high, making it difficult to develop unique methods for UHPLC-MS isolation and analysis.
- In all cases, these chemical species are present at very low concentrations. Consequently, other secondary metabolites present in higher concentrations, such as polyphenols, can cause matrix effects and represent significant interferences in signal generation (ion suppression processes in electrospray ionization (ESI)), while also complicating the acquisition of tandem mass spectra. Additionally, aliphatic glycoside compounds often exhibit markedly different and, frequently, low ionization yields, making their analysis more challenging.
- The diversity of molecules prevents them from being analysed using a single ionization mode.

These difficulties suggest that preconcentration and isolation processes will be important, not only for identification and characterisation tasks but also for the development of quantitative analytical methods.

To address these challenges, the main objective of this study is to develop a fractionation strategy involving a sequence of semi-preparative chromatographies, first by size exclusion and then by normal phase fractionation. Fractions will be hydrolysed in model wine, and a selected number of relevant varietal odorants will be quantified, while an untargeted UHPLC-MS approach based on a high resolution QTOF mass spectrometer, will be carried out in the original fractions. This approach will enable the individual isolation and identification of glycosidic precursors and the establishment of more definitive associations with the aromas they produce, whether by direct hydrolysis or molecular rearrangement processes. The expansion of the database of aromatic precursor molecules is essential for a better understanding of aroma development in the grape and for addressing challenges related to climate change.

This procedure will be applied to the 'Garnacha' grape variety. Although Garnacha is known for its resilience to high temperatures and drought, its aromatic precursors have not yet been studied. As climate change alters the ripening and harvest times of grapes, often increasing the sugar content and resulting alcohol levels in wines (Burney et al., 2013; Petropoulos et al., 2017; Resco et al., 2016), it is crucial to identify the glycosidic precursors in 'Garnacha' grapes in order to predict and manage wine aroma profiles in an ever-changing environment.

## 2. Materials and methods

A flowchart outlining the experimental process of this study can be found in Supplementary Material Figure I.

### 2.1. Reagents, standards, and solvents

Tartaric acid, ascorbic acid, and sodium chloride were supplied by Panreac (Barcelona, Spain). Lichrosolv® grade methanol, along with methanol and formic acid, both LC-MS grade, were supplied by Fisher Scientific (Loughborough, UK). Lichrosolv® grade ethanol, ammonium formate (LC-MS grade), 2-octanol (99.5 % purity), 3-octanone (99 % purity), 3,4-dimethylphenol (99 % purity), phenyl *β-D*-glucopyranoside (> 95 % purity), and octyl *β-D*-glucopyranoside (> 95 % purity) were

purchased from Merck (Darmstadt, Germany). Ethyl acetate (HPLC grade) was supplied by Scharlab (Barcelona, Spain). The chemical standards used for the analysis of minor volatile compounds (see Supplementary Material, Tables I-VIII) were supplied by Merck with a purity greater than 98 %, except for 1,1,6-trimethyl-1,2-dihydronaphthalene (TDN), which was synthesized by Synchem UG & Co (Felsberg, Germany) with a purity of 80 %. Pure water was obtained from a Milli-Q purification system (Millipore, Massachusetts, USA). Nitrogen (> 99.999 % *v*/v purity), hydrogen (> 99.999 % v/v purity), and helium (> 99.996 % v/v purity) were supplied by Air Liquide.

### 2.2. Fractionation

#### 2.2.1. Sample preparation

*2.2.1.1. Preparation of mistelles.* Twenty-seven 'Garnacha' mistelles were prepared from grapes of the 2022 vintage, comprising fifteen from Campo de Borja D.O. (Aragon region) and twelve from Rioja D.O.Ca. (La Rioja region). One kilogram of each 'Garnacha' grape sample was destemmed and placed in a large beaker, spiked with 50 mg $kg^{-1}$ of potassium metabisulfite, and gently crushed by hand. Subsequently, 190 mL $kg^{-1}$ of pure ethanol was added. The resulting mixture was transferred to a 1.5 L PET bottle, which was squeezed to displace the remaining air, and left to macerate for 2 weeks at 8 °C with daily manual agitation. After maceration, the supernatant was recovered, combined with the liquid obtained by pressing the solids, and allowed to settle for an additional week at 8 °C. Finally, the liquid (mistelle) was centrifuged at 3894 RCF and 4 °C for 10 min, and bottled in 1 L PET bottles, which were stored at 4 °C.

*2.2.1.2. Preparation of PAFs.* Phenolic-aromatic fractions (PAFs) were prepared from each of the mistelles (15 from Campo de Borja D.O. and 12 from Rioja D.O.Ca.), following the procedure described by Alegre et al. (2020) with some modifications. According to this, each mistelle, derived from 1 kg of 'Garnacha' grapes, was centrifuged at 3894 RCF and 10 °C for 15 min (AllegraTM, California, USA) and then diluted with Milli-Q water to standardize the maximum volume obtained among all the samples (830 mL per kg of grapes). This step was essential because yields varied among grape samples, making it necessary to ensure that all samples had a similar volume and alcohol content at the start of the de-alcoholisation process. After the dilution step, the samples were de-alcoholised in a rotary evaporator (Buchi R-215 equipped with a V-700 vacuum pump from Buchi, Flawil, Switzerland) to a final volume of 450 mL. Each de-alcoholised mistelle was then percolated through a 10 g Sep Pack C18 cartridge (Waters, Ireland) previously conditioned with 44 mL of methanol, followed by 44 mL of Milli-Q water with 2 % ethanol. Sugars, amino acids, and ions were removed by washing with 88 mL of Milli-Q water at pH 3.5. The polyphenolic and aromatic precursor fraction (PAF) was recovered by elution with 100 mL of absolute ethanol.

*2.2.1.3. Preparation of the 'Garnacha' PAF mixture.* A composite sample was prepared by mixing 2 mL from each of the 27 phenolic-aromatic fractions (15 from Campo de Borja D.O. and 12 from Rioja D.O.Ca.), giving a total volume of 54 mL.

*2.2.1.4. Preparation of synthetic wine mixtures for fractionation.* Aliquots with 18 mL of the 'Garnacha' PAF mixture were evaporated to dryness in a round-bottomed flask using a rotary evaporator. The resulting solid fractions were then redissolved in 18 mL of synthetic wine (12 % ethanol (*v*/v), 5 g $L^{-1}$ tartaric acid, and pH 3.5) to constitute the wine-like concentrated PAF.

#### 2.2.2. Fractionation using Toyopearl

This first fractionation step was carried out following the methodology described by Sáenz-Navajas et al. (2017) with some modifications. The aim of this step was to perform a preliminary separation using a semi-preparative Vantage L HW-50F column (Millipore, Bedford, MA), 280 mm in length and 44 mm in internal diameter, packed with Toyopearl gel (HW 50F) and operating at a flow rate of 10 mL $min^{-1}$. A total of 18 mL of the wine-like concentrated PAF were injected into the column, and the eluate was collected in four different fractions. The first fraction (T1) was made up of 2600 mL of ethanol/water/formic acid (55:45:1, *v*/v/v), the second fraction (T2) consisted of 770 mL of acetone. The third (T3) and fourth (T4) fractions were made up of 295 and 840 mL of acetone/water (80:20) and (60:40), respectively. Each of the four fractions was divided into two round-bottomed flasks, evaporated to a constant volume, and then lyophilised to dryness.

#### 2.2.3. Aroma-based selection of Toyopearl fractions

To identify which fractions collected from the Toyopearl column (T1-T4) would be selected for silica gel fractionation, each of the four fractions was redissolved in 18 mL of ethanol. From each, 1.5 mL was taken, evaporated to dryness using a rotary evaporator, and redissolved in 10 mL of synthetic wine (12 % ethanol v/v, pH 3.5, and 5 g $L^{-1}$ tartaric acid). The headspace of the vials was purged with $N_2$, and the samples were vacuum sealed in heat-sealed bags (Coimbra Pack S.L., Spain). Subsequently, acid hydrolysis was performed under anoxic conditions at 75 °C for 24 h (JP Selecta, Barcelona, Spain).

The resulting hydrolysates were subjected to sensory evaluation to assess the presence or absence of odorants. Sensory analyses were conducted in compliance with the Declaration of Helsinki. Accordingly, participants were informed at the beginning of the experiment that they would remain anonymous, that data provided would only be reported in the aggregate and that they had the rights to clarify any doubts by requesting more detailed information, to withdraw from the experiment at any time, to request access to their personal data from the data controller, to request any rectification, deletion, limitation in their processing and data portability, or any other rights that may correspond to them, and to withdraw their consent at any time by contacting the experimenters. Participants had to acknowledge an informed consent statement, had to be over 18 years of age and not present any pathology that could be incompatible with the sensory analysis, not be intolerant to alcohol, not be pregnant and not be directly linked to the research. They did not receive financial compensation for their participation. The sensory tasks were carried out by members of the LAAE laboratory staff who were very experienced in wine aroma description, had run wine-tasting classes, and had relevant professional experience in winemaking (Parr et al., 2002). A panel of six trained judges (3 men and 3 women, aged between 30 and 60 years), was asked to smell each of the four randomly ordered vials and indicate which fractions exhibited aromas, without rating intensity or providing descriptors. Fractions showing any aroma were selected for further analysis.

#### 2.2.4. Fractionation using a silica gel column

*2.2.4.1. Sample preparation.* The Toyopearl fractionation was repeated under the same chromatographic conditions using a second 18 mL aliquot of the wine-like concentrated PAF. For the selected fraction(s) presenting aroma, the contents of each of the two new lyophilised distillation flasks were dissolved in 9 mL of ethanol and then combined. The resulting 18 mL solution was evaporated to dryness in a rotary evaporator and redissolved in 5 mL of ethanol.

*2.2.4.2. Fractionation on silica gel.* The second fractionation step was performed by semi-preparative liquid chromatography using an Omnifit column (2.5 cm i.d. 45 cm) packed with silica gel 60 (Merck, Darmstadt, Germany) (particle size 0.04–0.06 mm). The column was operated at a flow rate of 8 mL $min^{-1}$ using a HPLC pump (Waters 510 HPLC Millipore, Bedford, MA). Twelve mobile phase (MP) compositions (150 mL

each) were prepared using ethyl acetate (A), methanol (B), Milli-Q water (C), and Milli-Q water adjusted to pH 1 (D). Each solution was filtered through 47 mm nylon filters (Fisher Scientific, Loughborough, UK) and sonicated for 5 min (JP Selecta, Barcelona, Spain). The 5 mL ethanol sample obtained from the previous step was loaded onto the column and a stepwise gradient was applied as follows (A%/B%/C%/D%): 100/0/0/0 (MP1), 95/5/0/0 (MP2), 90/10/0/0 (MP3), 80/20/00 (MP4), 60/40/0/0 (MP5), 20/80/0/0 (MP6), 0/100/0/0 (MP7), 0/95/5/0 (MP8), 0/85/15/0 (MP9), 0/50/50/0 (MP10), 0/0/100/0 (MP11), 0/0/0/100 (MP12). For each mobile phase composition, seven 20 mL fractions and one 10 mL fraction were collected. In total, 96 fractions were obtained, 8 for each mobile phase. In terms of sample coding, the first letter denotes silica gel fractionation, the first number indicates the mobile phase used during the silica fractionation (from MP1 to MP12), and the second number specifies the fraction collected for that mobile phase (from 1 to 8). For instance, "F4.1" means that the silica fraction was obtained using the mobile phase 4 (MP4) and corresponds to the first vial of this mobile phase.

### 2.3. Sensory selection of target fractions

Fractions were dried, reconstituted, hydrolysed and sensory assessed to select those developing aromas for GC–MS and HPLC-MS analysis as detailed in the next sections.

#### 2.3.1. Hydrolysis

Three millilitres of each fraction obtained from the silica gel fractionation process were dried. Fractions without water (MP1–7) were dried under a stream of $N_2$ using a multichannel evaporator (Reacti-Vap from Thermo Scientific, Massachusetts, USA). Fractions containing methanol and water (MP8–10) were rotary evaporated to remove methanol, then frozen and dried using a LyoQuest-85 lyophilisation system from Telstar (Terrassa, Spain). Fractions that were only in water (MP11–12) were frozen and lyophilised directly.

These dried fractions were reconstituted in 8 mL of synthetic wine (10 % ethanol (*v*/v), pH 3.5, and 5 g $L^{-1}$ tartaric acid) in 10 mL screw-capped vials (Análisis Vínicos S.L., Spain). The headspace of the vials was purged with $N_2$, and the samples were vacuum sealed in heat-sealed bags (Coimbra Pack S.L., Spain). The samples were then hydrolysed under anoxic conditions at 75 °C for 24 h. After this period, the samples were stored in a refrigerator at 5 °C until use.

#### 2.3.2. Sensory evaluation of hydrolysed fractions

The sensory evaluation of the hydrolysed fractions was performed by a panel of five trained judges (2 men and 3 women, aged between 22 and 60 years), selected and informed as detailed in Section 2.2.3, using a two-alternative forced choice test. The panellists were asked to identify the fractions that had a different aroma to the hydrolysed reference (8 mL of synthetic wine hydrolysed at 75 °C for 24 h). In addition, they were encouraged to describe the aromatic characteristics of the samples whenever possible, as these descriptors could assist in the subsequent identification of compounds. Fractions showing any aroma were selected for further analysis. For the evaluation, the samples were tempered and served in different sessions, with a random order for each judge.

### 2.4. SPME-GC–MS analysis of selected hydrolysed fractions

The analysis of the minor volatile compounds present in the sensorially selected fractions was performed by solid-phase microextraction with mass spectrometry detection (SPME-GC–MS), following the method described by Ferreira et al. (2015), with some modifications.

First, a saturated brine solution was prepared by mixing 350 g of NaCl, 1 L of Milli-Q water and 500 mg of ascorbic acid. The sample was prepared by mixing 1.7 mL of the hydrolysed fraction, 8.5 mL of brine, and 40 µL of an internal standard solution (2-octanol, 3-octanone, and 3,4-dimethylphenol, all at 0.5 mg $L^{-1}$) in a 20 mL screw cap vial (Análisis Vínicos S.L., Spain). Volatile compounds were extracted from the headspace using a divinylbenzene-carboxen-polydimethylsiloxane (DVB-CAR-PDMS) fibre with a 50/30 µm coating, 24-gauge, and 2 cm in length (Supelco, Bellefonte, USA), and analysed using a GC–MS (QP2010 Shimadzu, Japan) as described by Ferreira et al. (2015). Calibration was performed by response factors (RFs) calculated by analysing a synthetic wine solution containing known concentrations of the analytes (see Supplementary Material, Tables I-VIII).

### 2.5. UHPLC-QTOF-MS analysis of selected non-hydrolysed fractions

#### 2.5.1. Sample preparation

This analysis was performed on those fractions obtained from the silica gel fractionation (see section 2.2.4) whose hydrolysates contained the target varietal aromas (see section 2.4). For this purpose, 20 µL of an internal standard solution (phenyl *β-D*-glucopyranoside and octyl *β-D*-glucopyranoside, both at 15 mg $L^{-1}$) was added to 3 mL of each selected non-hydrolysed fraction. The samples were then evaporated to dryness under a nitrogen stream, redissolved in 200 µL of LC-MS grade methanol and filtered through 0.13 mm diameter, 0.22 µm pore size polytetrafluoroethylene (PTFE) syringe filters (FilterBio, Madrid, Spain), before being transferred to 200 µL insert vials.

In addition, a quality control sample (QC) was prepared by mixing equal volumes (56 µL) of the different selected fractions. The QC extract was processed in the same way as the samples. This QC was injected six times at the start of the analysis and then every ten samples to ensure correct chromatographic performance.

#### 2.5.2. Analysis by liquid chromatography coupled with quadrupole time-of-flight mass spectrometry (UHPLC-QTOF-MS)

7 µL of each sample were injected into a Bruker Daltonics UHPLC-TIMS-QTOF-MS system (Billerica, USA). Samples were kept at 4 °C in the autosampler throughout the analysis. Chromatographic separation was performed on a Waters C18 column (100 × 2.1 mm, 1.7 µm particle size; Milford, USA) maintained at 35 °C.

The flow rate was 0.3 mL $min^{-1}$, with Milli-Q water (phase A) and acetonitrile (phase B) as mobile phases, both containing 0.1 % formic acid. The chromatographic program was as follows: during the first 3.5 min, the mobile phase contained 5 % B; then, it was increased to 45 % B, which was reached at minute 8.7 of the analysis; followed by an increase to 65 % B, reached at minute 11.2; and finally, up to 90 % B, reached at minute 13.3 and maintained until minute 18.7. The fractions were analysed in negative ESI and MS mode, and selected samples and QC were also analysed in MS/MS mode. Nitrogen was used as the drying gas at a flow rate of 10 L $min^{-1}$ and a temperature of 220 °C. The nebuliser pressure was 2.2 bar, and the capillary voltage was 3600 V. These source conditions were consistent for both MS and MS/MS analyses. The mass range was *m/z* 50–1300, with a spectral acquisition rate of 12 spectra per second.

#### 2.5.3. Data processing

Data were processed using Bruker's Metaboscape software (Karlsruhe, Germany), and a global Feature Table (Arapitsas et al., 2016) was generated for all fractions and QC samples. In order to simplify the identification process, a main Target List containing expected exact masses of precursors was built by combining each one of the potential aglycones (Supplementary Material Table IX) previously reported (Barnaba et al., 2017; Barnaba, Dellacassa, et al., 2018; Barnaba, Larcher, et al., 2018; Caffrey et al., 2019, 2020; Flamini et al., 2014; Hjelmeland et al., 2015; Wei et al., 2021) with all possible mono, di and trisaccharides (Supplementary Material Table X). Additionally, the exact masses of their formate adducts (Caffrey et al., 2020; Wei et al., 2021) were also included. Such a Target List, containing more than 1000 expected exact masses was then applied to the experimental Feature Table to select those features with molecular formulas consistent with

potential precursors, with a mass error within ±5 ppm of the theoretical value.

MS/MS spectra from selected samples analysed by Data Independent Acquisition (DIA) were included to aid precursor identification.

Additional MS/MS spectra were acquired using Data Dependent Acquisition (DDA) for selected features with high intensity signals (> 50,000 counts) not captured by DIA. Scheduled Precursor Lists (SPL) were generated for these features, allowing MS/MS acquisition at defined intervals. Samples with the highest feature intensities were re-injected using the SPLs.

After importing the MS/MS spectra into the features, potential precursor structures were verified by identifying the fragments: $[M\text{-}H]^-$ and/or $[M + HCOOH\text{-}H]^-$ (formate adduct), the aglycone fragment, as well as those of simple sugars, disaccharides, and trisaccharides, and their neutral losses. The accepted mass error for experimental fragments was ±5 ppm relatives to theoretical values.

The correlation between precursor intensities in a consecutive set of original non-hydrolysed fractions (UHPLC-QTOF-MS) and corresponding aromatic concentrations (SPME-GC–MS) found in the equivalent set of hydrolysed fractions was determined.

## 3. Results and discussion

The systematic combination of C18, Toyopearl size-exclusion and silica-gel fractionation, together with complementary analytical techniques (targeted SPME-GC–MS and untargeted UHPLC–MS), has proven highly effective for the identification of glycosidic precursors. During C18 extraction, sugars, amino acids and ions, which can induce ion suppression in ESI, are removed. The subsequent Toyopearl size-exclusion step eliminates high-molecular-weight compounds that can cause matrix effects and further ion suppression, while silica gel fractionation enables the isolation and preconcentration of glycosidic precursors. Moreover, the integrated analysis of aroma compounds by GC–MS and precursors by UHPLC–MS allows for the determination of which precursors exert the greatest influence on the aromatic profile, as will be detailed in the following sections.

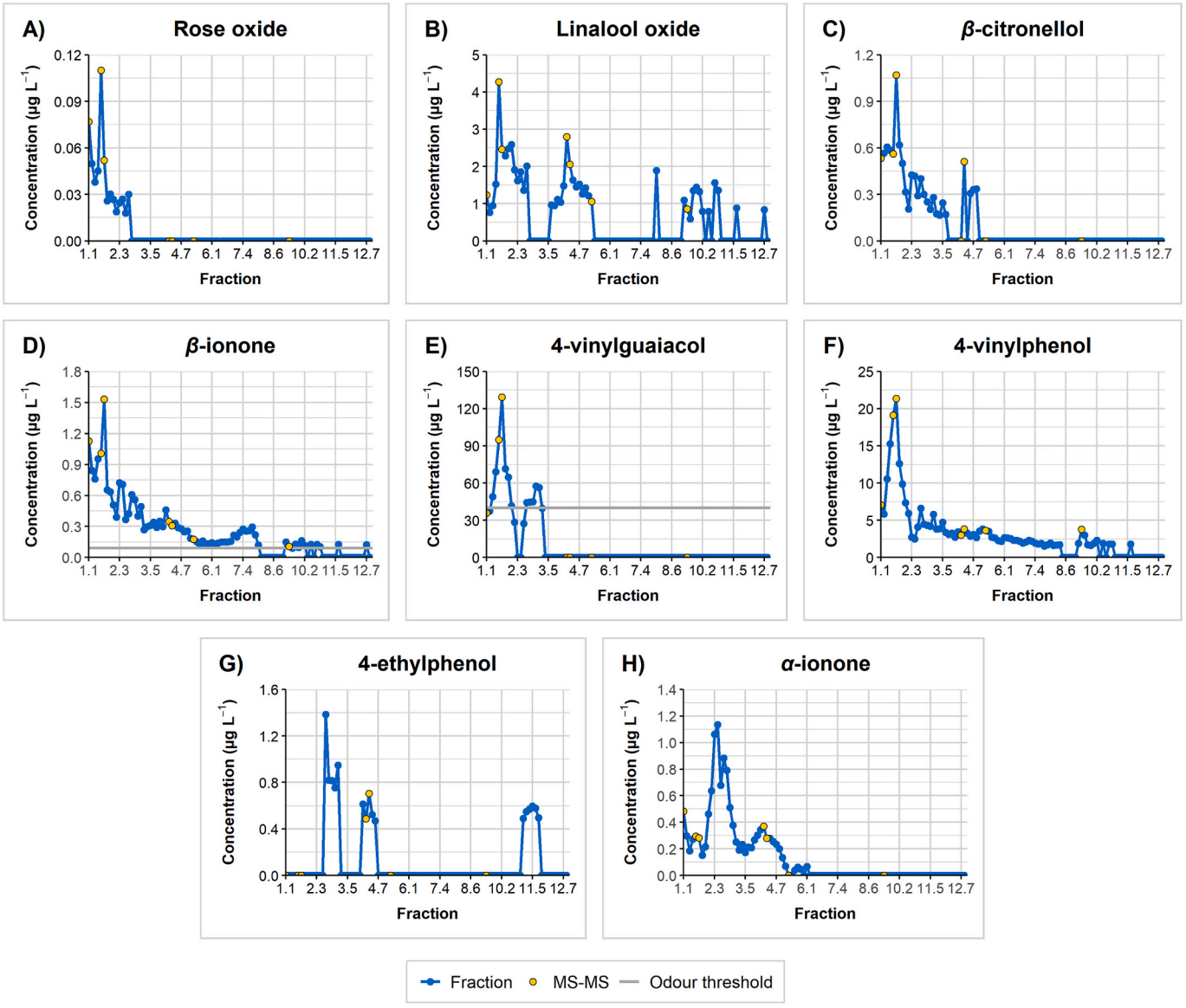


**Fig. 1.** Distribution profile of: A) rose oxide, B) linalool oxide, C) *β*-citronellol, D) *β*-ionone, E) 4-vinylguaiacol, F) 4-vinylphenol, G) 4-ethylphenol, and H) *α*-ionone in the different fractions. Error bars have been omitted to make the image easier to read. (For interpretation of the references to colour in this figure legend, the reader is referred to the web version of this article.)

### 3.1. Sensory analysis

*Aroma-based selection of Toyopearl fractions*: Among the four fractions obtained from the Toyopearl fractionation, only T1, containing low molecular mass compounds, developed aroma after hydrolysis. This implies that all aroma precursors are small metabolites. This T1 fraction was selected for subsequent fractionation using silica gel.

*Aroma-based selection of Silica fractions:* Sensory analysis of the 96 hydrolysed fractions obtained from the silica gel fractionation, carried out as described in section 2.3, revealed that four of them (F6.5, F9.7, F10.1, and F10.7) did not develop an aroma. The 92 aromatic fractions were therefore selected for SPME-GC–MS analysis.

### 3.2. SPME-GC–MS analysis

Figs. 1–3 show the concentrations of aroma molecules measured in each of the 92 hydrolysed fractions analysed by SPME-GC–MS (blue line). Odour thresholds (San-Juan et al., 2012) are represented by a grey line while the fractions selected for untargeted analysis (DIA) by UHPLC-QTOF-MS/MS are marked with a yellow dot. The complete quantitative data can be found in Supplementary Material (Tables I–VIII).

The distribution profiles of the aroma molecules in the fractions reveal that aroma precursors elute in three main elution zones. The first corresponds to the mobile phase with the lowest elution strength (MP1). In this region, certain terpenes (rose oxide, linalool oxide, and $\beta$-citronellol, Figs. 1 A-C, respectively), a norisoprenoid ($\beta$-ionone, Fig. 1 D), as well as some phenols (4-vinylphenol and 4-vinylguaiacol, Figs. 1 E and F, respectively) are mainly eluted. These compounds reach their maximum concentration around F1.5-F1.6.

In Fig. 1 G-H, a second region is observed around MP2 and MP3, where 4-ethylphenol (a phenol, Fig. 1 G) and $\alpha$-ionone (a norisoprenoid, Fig. 1 H) predominantly elute.

The third region is observed around MP4 and MP5 (Fig. 2). In this zone, norisoprenoids ($\beta$-damascenone, Riesling acetal, TDN, and vitispiranes, as seen in Figs. 2 A-D, respectively), certain terpenes (geraniol, linalool, and $\alpha$-terpineol, Figs. 2 E-G, respectively), and phenols (syringol and guaiacol, Figs. 2 H and I, respectively) are concentrated.

Ethyl cinnamate and ethyl dihydrocinnamate (Figs. 3 A and B, respectively) have the particularity of being found in isolated fractions: ethyl cinnamate is present in F1.1, F1.3, and F9.3, while ethyl

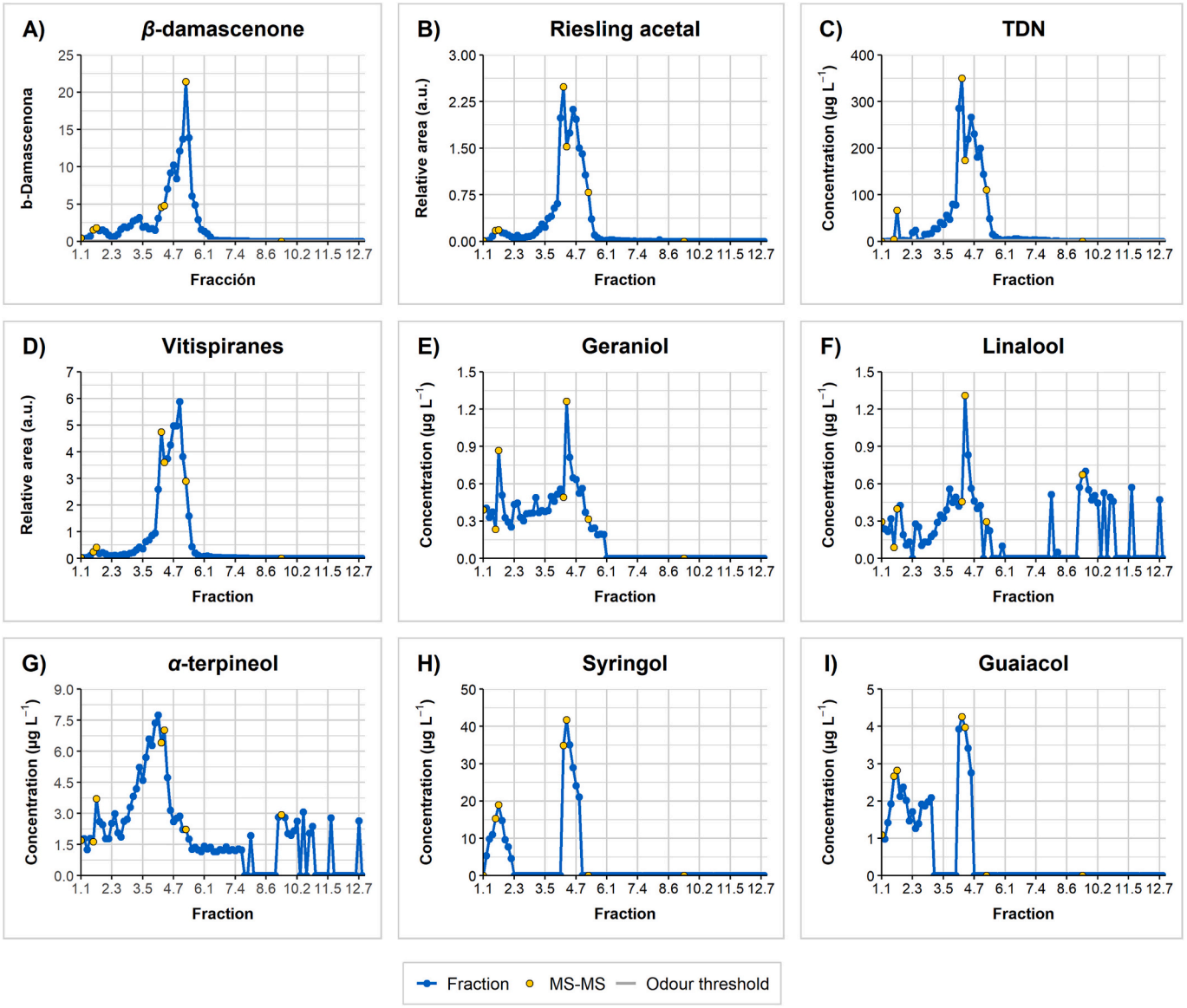


**Fig. 2.** Distribution profile of: *A)* $\beta$-damascenone, B) Riesling acetal, C) TDN, D) vitispiranes, E) geraniol, F) linalool, G) $\alpha$-terpineol, H) syringol and I) guaiacol in the different fractions. Error bars have been omitted to make the image easier to read.

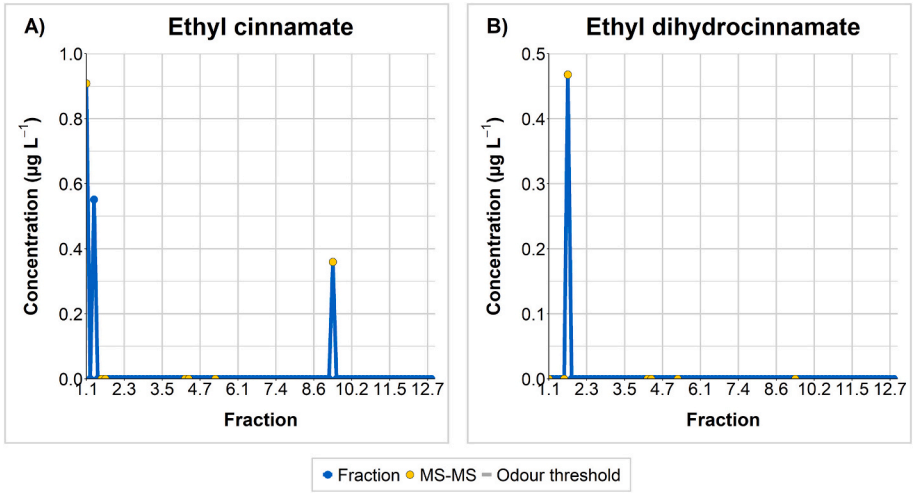


**Fig. 3.** Distribution profile of: A) ethyl cinnamate and B) ethyl dihydrocinnamate in the different fractions. Error bars have been omitted to make the image easier to read.

dihydrocinnamate is found in F1.6. Despite their low concentrations, this observation suggests the existence of precursors with a notable difference in polarity in the case of ethyl cinnamate.

As can be seen, several aromas were found in more than one region. This is the case for linalool oxide (second peak in F4.3, Fig. 1 B) and some norisoprenoids such as $\alpha$-ionone (second peak in F1.1 and third peak in F4.3, Fig. 1H) and TDN (second peak in F1.6, Fig. 2 C). This was particularly evident for phenols, such as 4-vinylguaiacol (second peak in F3.2, Fig. 1 E), 4-ethylphenol (second peak in F4.4 and third peak in F11.6, Fig. 1 G), syringol (second peak in F1.6, Fig. 2 H), guaiacol (second peak in F1.6, Fig. 2 I), and also for geraniol (second peak in F1.6, Fig. 2 E).

The presence of the same compound in different fractionation regions indicates the existence of precursors of the same analyte with distinct structures, either in the aglycone or the glycosidic part. In any case, these precursors exhibit sufficiently different polarities to allow their separation in the silica gel column.

### 3.3. *UHPLC-QTOF-MS analysis*

The distribution profiles of the targeted varietal aromas (Figs. 1–3) revealed that their precursors were present in F1.1–F7.6, as well as in F9.3. For this reason, only 55 out of the 92 fractions were analysed using UHPLC-QTOF-MS, along with the QC (mixture of all the analysed

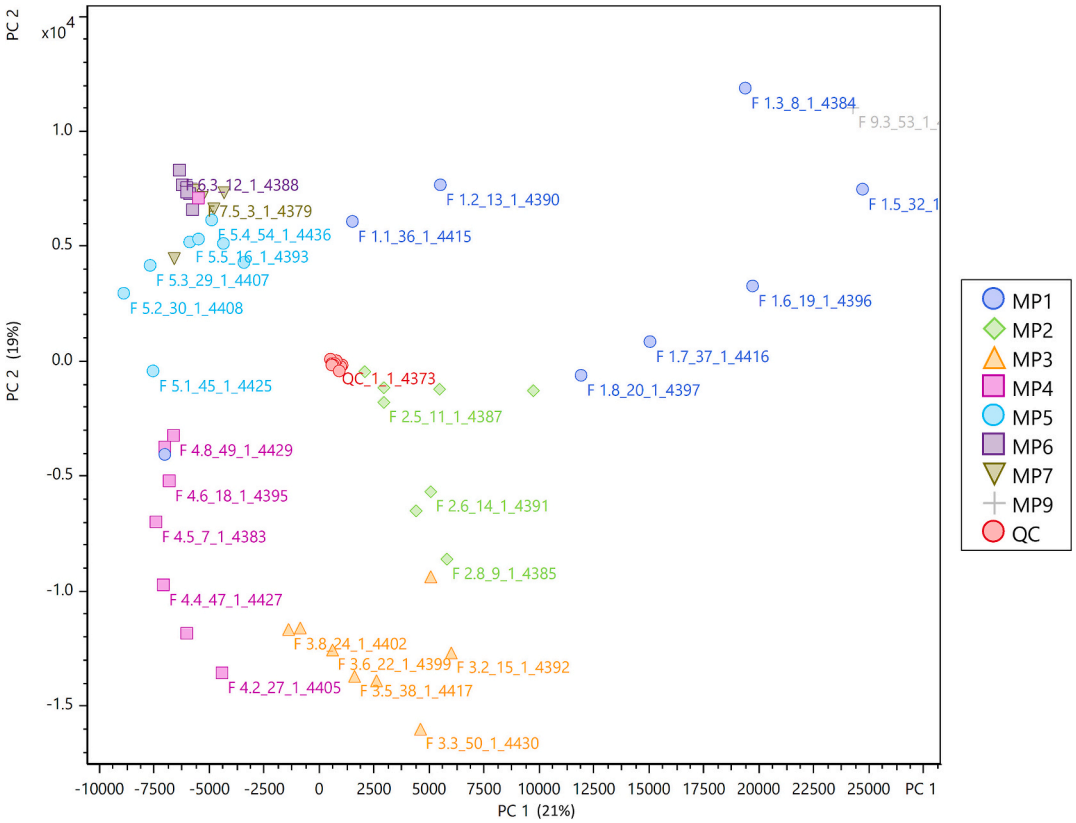


**Fig. 4.** Principal component analysis of all samples and QC for UHPLC-QTOF-MS.

fractions). Additionally, the fractions with the highest or near-maximum concentrations of aromatic compounds, as determined by SPME-GC–MS (fractions: F1.1, F1.5, F1.6, F4.3, F4.4, F5.3, and F9.3), were analysed using UHPLC-QTOF-MS-MS with the DIA strategy. The QC sample was also analysed using this acquisition strategy because, being an average sample of all fractions, it could include MS-MS spectra of precursors present in some of the fractions not included in the previous set. The analysed fractions contained the three main elution zones of MP1, MP4, and MP5, as well as F9.3 for its ethyl cinnamate content.

### 3.3.1. Data processing

The data processing for the 55 analysed samples (F1.1–7.6 and F9.3) and the QC resulted in a global Feature Table containing 90,922 features. Using the intensities of these features across all fractions and the QC, a principal component analysis (PCA) was performed. Fig. 4 shows the distribution of the fractions and the QC in the PCA. The first two PCs accounted for almost 40 % of the original variance. The first PC explained 21 % of the original variance, whereas the second factor represented 19 %. As can be seen, the fractions are scattered throughout the PCA according to their composition. They start in the second quadrant with MP1, which contains 100 % ethyl acetate. They then move clockwise as the amount of ethyl acetate decreases and the amount of methanol increases. They end in the first quadrant with 100 % methanol (MP7). This behaviour is consistent with expectations, as the fractions clustered according to the mobile phase with which they were eluted. Adjacent fractions tend to exhibit similar compound profiles because they were eluted with mobile phases of comparable elution strengths. It can also be seen that the QC is centrally located, verifying its average concentration and confirming the consistency of the process.

On this global Feature Table of 90,922 features, the Target List containing more than 1000 exact masses of the ions expected to be formed from potential aroma precursors (section 2.5), was applied in order to select the features congruent with those masses. With this operation, the number of features retained for subsequent analysis was significantly reduced to 7606 in the Feature Table “A”. Next, MS-MS spectra obtained through the two acquisition strategies (DIA and DDA) were imported onto this reduced Feature Table “A” to assign fragmentation mass spectra of parent ions that would help in the identification of the precursors. Using these spectra, the target feature list was further reduced to 858 in the Feature Table “B.” Then, the congruence between the experimental MS/MS fragmentation and the most likely molecular structure assigned to that exact mass was manually assessed. Finally, the determination coefficients ($R^2$) between the intensities of the features measured in a set of consecutive LC fractions, and the concentrations of the corresponding aromatic compounds measured in the corresponding hydrolysed fractions, were calculated as an additional identity criterion. These premises made it possible to produce the Feature Table “C”, with 373 potential precursors, grouped into four categories based on the confidence level in their identification: Category 1, consistent MS-MS and $R^2 > 0.7$; Category 2, consistent MS-MS, but correlation could not be assessed; Category 3, consistent MS-MS, $R^2 < 0.7$; Category 4, inconsistent MS-MS, $R^2 > 0.7$. The knowledge about the real identity of the potential precursors included in the 4th category was considered to be insufficient, so this category was excluded from the final Feature Table, which was Feature Table “D” containing the 185 features from the first three categories, as shown in Table 1. Precursors in the table are ordered by category (marked as Cat) and then, by retention time. The mobile phases (MP) in which the precursors were found in the preparative fractionation (marked as MP), their exact masses, the fragments found in the MS-MS analysis (aglycone or other fragments), and the determination coefficients are also included in the table.

Of the 185 identified precursors, 111 are distinct, while the remaining 74 have the same glycone-aglycone structure as some of the other 111, and cannot be distinguished from the obtained spectrometric data. This happens, for example, in molecules with the same sugar combination, such as hexose-pentose, since the analytical method used cannot differentiate between the different hexoses and pentoses. Of these, 98 had not been previously described in the literature. Precursors with the same glycone-aglycone structure will be referred as of the same type, and in the following sections are shown with the symbol “≈” between them.

Aromatic precursors often exhibit characteristic fragmentation patterns, typically involving the loss of sugar moieties. In some cases, this loss directly releases the aroma compound, while in others, such as ipsdienol or geranic acid, the resulting molecule undergoes rearrangement to form the specific terpenes (e.g., linalool, $\alpha$-terpineol, geraniol and nerol).

### 3.3.2. Precursors with consistent MS-MS and significant aroma correlation (category 1)

There are 75 compounds in this category, including precursors of terpenes, norisoprenoids, and some volatile phenols. As can be observed in Table 1, in quite a limited number of cases it has been possible to obtain MS-MS fragments corresponding exclusively to the aglycone. Furthermore, in some cases, a single ion corresponding to a free sugar was found. This limitation is general to many precursors listed in Table 1.

*3.3.2.1. Potential terpene precursors.* For the terpene family, 54 potential precursors corresponding to 37 different types were identified. Among these are five trisaccharides of ipsdienol (no. 3 ≈ 10 ≈ 43, 9 ≈ 48, where the number refers to the column marked with the symbol #); seven precursors of monoterpenol: six trisaccharides (no. 53, 56, 57, 61 ≈ 66, 68) and one disaccharide (no. 64); eight precursors of monoterpendiol, two of which are trisaccharides (no. 4, 36) and six are disaccharides (no. 16 ≈ 34 ≈ 50, 32 ≈ 39, 72); two precursors of dihydromonoterpendiol, one trisaccharide (no. 7) and one disaccharide (no. 33); four disaccharides of dihydromonoterpentriol (no. 14 ≈ 21 ≈ 46 ≈ 49); four precursors of dehydromonoterpentriol: two disaccharides (no. 6, 28) and two trisaccharides (no. 40 ≈ 69); two trisaccharides of monoterpentriol (no. 25 ≈ 37), and three precursors of dihydromonoterpentetraol: two disaccharides (no. 8 ≈ 42) and one trisaccharide (no. 63).

Additionally, six precursors of citronellol or its isomer, dihydromyrcenol, were identified: three trisaccharides (no. 15, 44, 60) and three disaccharides (no. 20 ≈ 38, 62); seven precursors of hydroxycitronellol: four disaccharides (no. 23 ≈ 52, 45, 73) and three trisaccharides (54, 74 ≈ 75); and six precursors of geranic acid: three trisaccharides (no. 5, 27, 51) and three disaccharides (no. 47 ≈ 65, 71).

These precursors were identified in MP4 and MP5 and were primarily correlated with linalool oxide, geraniol, and $\alpha$-terpineol, all of them aroma compounds whose first or second maxima were located around these fractions (Figs. 1 B, 2 E, and 2 G, respectively). This suggests that these precursors constitute major contributors to the formation of these aroma compounds. Notably, several of these precursors (no. 16 ≈ 34 ≈ 50, 32 ≈ 39, 33, 36, 45, 47 ≈ 65, 64, 71 and 72) have been previously reported by Caffrey et al. (2020), Wei et al. (2021), and/or Ghaste et al. (2015) in comprehensive studies of glycosidic aroma precursors involving different grape varieties (e.g., Riesling, Muscat, Sauvignon Blanc, Chardonnay, etc.).

*3.3.2.2. Potential norisoprenoid precursors.* A total of 18 different potential precursors of norisoprenoids, of 12 different types, were identified in Category 1. It should be noted that, of the various norisoprenoids analysed using the SPME-GC–MS method, only Riesling acetal has a free hydroxyl group that allows the formation of glycosidic bonds and, therefore, it is the only one that presents direct glycosidic precursors. The other aromatic molecules, such as $\beta$-damascenone, TDN, vitispiranes and $\alpha$- and $\beta$-ionone, require molecular rearrangement processes of their precursors to be formed. Aglycones of the precursors of

**Table 1**
Potential precursors identified in the fractions for Feature Table "D".

| # | Cat[a] | MP[b] | $t_r^c$ (min) | Precursor and molecular formula | *m/z* exp[d] M exp[e] | Mass error[f] | Fragments MS-MS spectrum | | Coefficient of determination[g] |
|---|---|---|---|---|---|---|---|---|---|
| | | | | | | | Aglycone | Other fragments | |
| 1 | 1 | 4 | 6.08 | guaiacol-hexose-hexose[1] ($C_{19}H_{28}O_{12}$) | 447.15060 448.15788 | 0.77 | 123.04500 | | guaiacol 0.76 |
| 2 | 1 | 4 | 6.37 | guaiacol-pentose-hexose[1–2] ($C_{18}H_{26}O_{11}$) | 417.14014 418.14742 | 1.08 | 123.04557 | 285.09814 [M-H-pentose+$H_2O$]$^-$ 255.08661 [M-H-hexose+$H_2O$]$^-$ 131.03454 [Pentose-H-$H_2O$]$^-$ 591.26582 [M-H]$^-$ | guaiacol 0.77 |
| 3 | 1 | 4–5 | 6.37 | ipsdienol-hexose-hexose-deoxypentose 1 ($C_{27}H_{44}O_{14}$) | 637.27093 592.27263 | 0.26 | | 429.21285 [M-H-hexose+$H_2O$]$^-$ 161.04464 [Hexose-H-$H_2O$]$^-$ 249.14842 [M-H-hexose-hexose]$^-$ | MP4: $\alpha$-terpineol 0.93 MP5: linalool oxide 0.97; geraniol 0.87; $\alpha$-terpineol 0.86 |
| 4 | 1 | 5 | 6.44 | monoterpendiol-hexose-pentose-pentose 1 ($C_{26}H_{44}O_{15}$) | 595.26041 596.26769 | 0.35 | | 179.05618 [Hexose-H]$^-$ 149.04514 [Pentose-H]$^-$ | linalool oxide 0.97; $\alpha$-terpineol 0.82; geraniol 0.78 |
| 5 | 1 | 4–5 | 6.92 | geranic acid-pentose-pentose-pentose ($C_{25}H_{40}O_{14}$) | 563.23388 564.24116 | 0.19 | | 149.04528 [Pentose-H]$^-$ | MP4: $R^2 < 0.7$ MP5: linalool oxide 0.76; $\alpha$-terpineol 0.53 |
| 6 | 1 | 4–5 | 7.04 | dehydromonoterpentriol-pentose-deoxypentose ($C_{20}H_{32}O_{10}$) | 431.19192 432.19920 | 0.45 | | 165.09233 [M-H-pentose-deoxypentose]$^-$ | MP4: $R^2 < 0.7$ MP5: geraniol 0.84 |
| 7 | 1 | 5 | 7.04 | dihydromonoterpendiol-hexose-pentose-pentose ($C_{26}H_{46}O_{15}$) | 597.27579 598.28307 | 0.10 | | 161.04571 [Hexose-H-$H_2O$]$^-$ | linalool oxide 0.89 |
| 8 | 1 | 5 | 7.06 | dihydromonoterpenetraol-hexose-hexose 1 ($C_{22}H_{40}O_{14}$) | 527.23419 528.24147 | 0.39 | | 347.17176 [M-H-hexose+$H_2O$]$^-$ | linalool oxide 0.91; geraniol 0.90; $\alpha$-terpineol 0.81 |
| 9 | 1 | 4–5 | 7.06 | ipsdienol-deoxyhexose-pentose-pentose 1 ($C_{26}H_{42}O_{13}$) | 561.25486 562.26213 | 0.25 | | 149.04514 [Pentose-H]$^-$ 131.03439 [Pentose-H-$H_2O$]$^-$ | MP4: $R^2 < 0.7$ MP5: linalool oxide 0.94; geraniol 0.92; $\alpha$-terpineol 0.87 |
| 10 | 1 | 4–5 | 7.10 | ipsdienol-hexose-hexose-deoxypentose 2 ($C_{27}H_{44}O_{14}$) | 637.27104 592.27242 | 0.43 | | 591.26485 [M-H]$^-$ 429.21323 [M-H-hexose+$H_2O$]$^-$ 161.04565 [Hexose-H-$H_2O$]$^-$ | MP4: $\alpha$-terpineol 0.88 MP5: linalool oxide 0.96; geraniol 0.90; $\alpha$-terpineol 0.88 |
| 11 | 1 | 4–5 | 7.11 | hydroxy-norisoprenoid group G-hexose-hexose 1[3–4] ($C_{25}H_{44}O_{14}$) | 567.26395 568.27122 | 2.35 | | 161.04500 [Hexose-H-$H_2O$]$^-$ | MP4: $\beta$-damascenone 0.90; $\alpha$-ionone 0.82 MP5: TDN 0.95; Riesling acetal 0.94; vitispiranes 0.93; $\beta$-ionone 0.85 |
| 12 | 1 | 4–5 | 7.11 | norisoprenoid group *E*-pentose-hexose[3,5–6] ($C_{24}H_{38}O_{12}$) | 563.23393 518.23546 | 0.10 | 223.13243 | 517.22770 [M-H]$^-$, 293.08766 [Pentose-hexose-$H_2O$]$^-$, 205.12299 [M-H-pentose-hexose]$^-$, 161.04512 [Hexose-H-$H_2O$]$^-$, 149.04546 [Pentose-H]$^-$, 131.03453 [Pentose-H-$H_2O$]$^-$ | MP4: $R^2 < 0.7$ MP5: TDN 0.92; Riesling acetal 0.92; vitispiranes 0.91; $\beta$-ionone 0.83 |
| 13 | 1 | 2–3 | 7.17 | norisoprenoid group E-hexose 1[3–4,6–7] ($C_{19}H_{30}O_8$) | 431.19202 386.19384 | 0.68 | | 385.18601 [M-H]$^-$ 205.12364 [M-H-hexose]$^-$ | MP2: $\beta$-damascenone 0.87 MP3: $\alpha$-ionone 0.76 |
| 14 | 1 | 4 | 7.17 | dihydromonoterpentriol-hexose-hexose 1 ($C_{22}H_{40}O_{13}$) | 511.23777 512.24504 | 2.54 | | 179.05562 [Hexose-H]$^-$ 161.04549 [Hexose-H-$H_2O$]$^-$ | dihydromyrcenol 0.75 |
| 15 | 1 | 4–5 | 7.17 | citronellol/dihydromyrcenol-hexose-pentose-pentose ($C_{26}H_{46}O_{14}$) | 581.28081 582.28809 | 0.22 | | 161.04527 [Hexose-H-$H_2O$]$^-$ | MP4: $\alpha$-terpineol 0.92 MP5: linalool oxide 0.96; geraniol 0.90; $\alpha$-terpineol 0.87 |
| 16 | 1 | 4–5 | 7.19 | monoterpendiol-pentose-hexose 1[3–11] ($C_{21}H_{36}O_{11}$) | 509.22351 464.22527 | 0.18 | | 463.21746 [M-H]$^-$ 347.16907 [M + HCOOH-H-hexose+$H_2O$]$^-$ | MP4: $R^2 < 0.7$ MP5: geraniol 0.95; linalool oxide 0.85; $\alpha$-terpineol 0.83 |
| 17 | 1 | 4 | 7.19 | norisoprenoid Group F-hexose[3–4] ($C_{19}H_{32}O_8$) | 433.20707 388.20900 | 0.70 | 225.14869 | 387.20189 [M-H]$^-$ 207.13713 [M-H-Hexose]$^-$ | $\beta$-ionone 0.82 |
| 18 | 1 | 5 | 7.21 | norisoprenoid Group F-pentose-hexose 1 ($C_{24}H_{40}O_{12}$) | 565.24971 520.25152 | 0.13 | | 519.24370 [M-H]$^-$ 387.20331 [M-H-pentose+$H_2O$]$^-$ | TDN 0.94; Riesling acetal 0.93; vitispiranes 0.91; $\beta$-ionone 0.82 |

(*continued on next page*)

**Table 1** (*continued*)

| # | Cat[a] | MP[b] | $t_r^c$ (min) | Precursor and molecular formula | *m/z* exp[d] M exp[e] | Mass error[f] | Fragments MS-MS spectrum | | Coefficient of determination[g] |
|---|---|---|---|---|---|---|---|---|---|
| | | | | | | | Aglycone | Other fragments | |
| 19 | 1 | 4–5 | 7.23 | hydroxy-norisoprenoid group G-hexose-hexose $2^{3-4}$ ($C_{25}H_{44}O_{14}$) | 567.26378 568.27106 | 2.65 | | 387.20035 [M-H-hexose]$^-$ 225.14769 [M-H-hexose-hexose]$^-$ 179.05645 [Hexose-H]$^-$ 161.04515 [Hexose-H-$H_2O$]$^-$ | MP4: $\beta$-damascenone 0.91; $\alpha$-ionone 0.81 MP5: Riesling acetal 0.89; TDN 0.88; vitispiranes 0.84 |
| 20 | 1 | 5 | 7.24 | citronellol/dihydromyrcenol-hexose-hexose 1 ($C_{22}H_{40}O_{11}$) | 479.24965 480.25692 | 0.86 | | 317.19733 [M-H-hexose+$H_2O$]$^-$ 299.18626 [M-H-hexose]$^-$ | linalool oxide 0.84 |
| 21 | 1 | 5 | 7.24 | dihydromonoterpentriol-hexose-hexose 2 ($C_{22}H_{40}O_{13}$) | 511.23850 512.24577 | 1.11 | | 179.05562 [Hexose-H]$^-$ 161.04549 [Hexose-H-$H_2O$]$^-$ | geraniol 0.92; linalool oxide 0.89; $\alpha$-terpineol 0.83 |
| 22 | 1 | 4 | 7.26 | norisoprenoid group F-pentose-hexose 2 ($C_{24}H_{40}O_{12}$) | 565.24929 520.25111 | 0.61 | | 519.24256 [M-H]$^-$ 387.20331 [M-H-pentose+$H_2O$]$^-$ | Riesling acetal 0.75 |
| 23 | 1 | 4–5 | 7.34 | hydroxycitronellol-hexose-deoxyhexose 1 ($C_{22}H_{42}O_{11}$) | 481.26476 482.27204 | 0.27 | | 319.21244 [M-H-hexose+$H_2O$]$^-$ | MP4: $\alpha$-terpineol 0.86 MP5: linalool oxide 0.96; $\alpha$-terpineol 0.84; geraniol 0.83 |
| 24 | 1 | 4–5 | 7.36 | norisoprenoid group C-hexose-hexose ($C_{25}H_{44}O_{12}$) | 581.28108 536.28269 | 0.25 | | 535.27486 [M-H]$^-$ 161.04542 [Hexose-H-$H_2O$]$^-$ | MP4: $\alpha$-ionone 0.79; $\beta$-damascenone 0.75 MP5: TDN 0.96; Riesling acetal 0.95; vitispiranes 0.94; $\beta$-ionone 0.85 |
| 25 | 1 | 4–5 | 7.38 | monoterpentriol-pentose-pentose-hexose 1 ($C_{26}H_{44}O_{16}$) | 611.25511 612.26238 | 0.01 | | 449.20438 [M-H-hexose+$H_2O$]- 431.19331 [M-H-hexose]$^-$ 329.15943 [M-H-pentose-pentose]- | MP4: $\alpha$-terpineol 0.87 MP5: linalool oxide 0.95; geraniol 0.87; $\alpha$-terpineol 0.83 |
| 26 | 1 | 5 | 7.43 | norisoprenoid group F-pentose-hexose 3 ($C_{24}H_{40}O_{12}$) | 565.24965 520.25147 | 0.03 | | 519.24364 [M-H]$^-$ 387.20331 [M-H-pentose+$H_2O$]$^-$ | Riesling acetal 0.92; TDN 0.92; vitispiranes 0.89 |
| 27 | 1 | 5 | 7.47 | geranic acid-pentose-pentose-deoxyhexose ($C_{26}H_{42}O_{14}$) | 577.24974 578.25701 | 0.18 | | 131.03425 [Pentose-H-$H_2O$]$^-$ 163.06141 [Deoxyhexose-H]$^-$ | linalool oxide 0.94; geraniol 0.91; $\alpha$-terpineol 0.87 |
| 28 | 1 | 1, 4–5 | 7.51 | dehydromonoterpentriol-pentose-hexose ($C_{21}H_{34}O_{12}$) | 523.20312 478.20476 | 0.83 | 183.10186 | 477.19782 [M-H]$^-$ 131.03464 [Pentose-H]- | MP1: $R^2 < 0.7$ MP4: $R^2 < 0.7$ MP5: linalool oxide 0.93; geraniol 0.92; $\alpha$-terpineol 0.85; dihydromyrcenol 0.72 |
| 29 | 1 | 1–5 | 7.51 | norisoprenoid group A-hexose-deoxyhexose[6] ($C_{25}H_{40}O_{11}$) | 561.25483 515.25665 | 0.20 | | 514.24882 [M-H]$^-$ 188.12689 [M-H-hexose-deoxyhexose]$^-$ 161.04484 [Hexose-H + $H_2O$]$^-$ | MP 1: $R^2 < 0.7$ MP2: $\beta$-damascenone 0.74 MP3: Riesling acetal 0.90; vitispiranes 0.89; TDN 0.83 MP4: $\beta$-ionone 0.81 MP5: TDN 0.92; Riesling acetal 0.91; vitispiranes 0.89 |
| 30 | 1 | 4 | 7.51 | norisoprenoid group *E*-hexose $2^{3-4,6-7}$ ($C_{19}H_{30}O_8$) | 431.19187 386.19372 | 0.34 | 223.13463 | 385.18641 [M-H]$^-$ 205.12395 [M-H-hexose]$^-$ | $\beta$-ionone 0.86 |
| 31 | 1 | 4–5 | 7.51 | norisoprenoid group F-hexose-deoxyhexose ($C_{25}H_{42}O_{12}$) | 579.26527 534.26708 | 0.03 | 225.14945 | 533.25925 [M-H]$^-$, 387.20091 [M-H-deoxyhexose+$H_2O$]$^-$, 307.10383 [Hexose-deoxyhexose-H-$H_2O$]$^-$, 207.13830 [M-H-hexose-deoxyhexose]$^-$, 163.06126 [Deoxyhexose-H]$^-$,161.04570 [Hexose-H-$H_2O$]$^-$ | MP4: $\beta$-damascenone 0.93 MP5: Riesling acetal 0.96; TDN 0.96; vitispiranes 0.94; $\beta$-ionone 0.82 |
| 32 | 1 | 4 | 7.59 | monoterpendiol-hexose-deoxyhexose $1^3$ ($C_{22}H_{38}O_{11}$) | 523.23913 478.24094 | 0.11 | | 477.23367 [M-H]$^-$ 163.06076 [Deoxyhexose-H]$^-$ | linalool oxide 0.73 |
| 33 | 1 | 4–5 | 7.67 | dihydromonoterpendiol-pentose-hexose[3,6–7,9,11] ($C_{21}H_{38}O_{11}$) | 511.23887 466.24080 | 0.39 | | 465.23339 [M-H]$^-$, 333.19224 [M-H-pentose+$H_2O$]$^-$, 331.17673 [M-H-hexose]$^-$, 179.05551 [Hexose-H]$^-$,161.04524 | MP4: $R^2 < 0.7$ MP5: linalool oxide 0.88 |

(*continued on next page*)

**Table 1** (*continued*)

| # | Cat[a] | MP[b] | $t_r^c$ (min) | Precursor and molecular formula | *m/z* exp[d] M exp[e] | Mass error[f] | Fragments MS-MS spectrum | | Coefficient of determination[g] |
|---|---|---|---|---|---|---|---|---|---|
| | | | | | | | Aglycone | Other fragments | |
| 34 | 1 | 5 | 7.67 | monoterpendiol-pentose-hexose $2^{3–11}$ ($C_{21}H_{36}O_{11}$) | 509.22410 464.22591 | 1.34 | | [Hexose-H + $H_2O$]$^-$, 149.04519 [Pentose-H]$^-$, 131.03395 [Pentose-H-$H_2O$]$^-$ 463.21808 [M-H]$^-$, 331.17547 [M-H-pentose+$H_2O$]$^-$, 179.05476 [Hexose-H], 161.04534 [Hexose-H-$H_2O$]$^-$ | geraniol 0.93; linalool oxide 0.92; $\alpha$-terpineol 0.85 |
| 35 | 1 | 5 | 7.70 | norisoprenoid group E-hexose-hexose 1 ($C_{25}H_{40}O_{13}$) | 547.23941 548.24668 | 0.62 | | 161.04441 [Hexose-H-$H_2O$]$^-$ | TDN 0.95; Riesling acetal 0.95; vitispiranes 0.92 |
| 36 | 1 | 5 | 7.72 | monoterpendiol-hexose-hexose-pentose[6] ($C_{27}H_{46}O_{16}$) | 671.27613 626.27794 | 0.17 | | 625.27011 [M-H]$^-$ 463.21856 [M-H-hexose+$H_2O$]$^-$ 331.17664 [M-H-pentose-hexose+$H_2O$]$^-$ | linalool oxide 0.93 |
| 37 | 1 | 4 | 7.72 | monoterpentriol-pentose-pentose-hexose 2 ($C_{26}H_{44}O_{16}$) | 611.25466 612.26194 | 0.74 | | 179.05589 [Hexose-H]$^-$ | $\alpha$-terpineol 0.72 |
| 38 | 1 | 4–5 | 7.74 | citronellol/dihydromyrcenol-hexose-hexose 2 ($C_{22}H_{40}O_{11}$) | 525.25454 480.25635 | 0.34 | | 479.24850 [M-H]$^-$ 345.19154 [M + HCOOH-H-hexose]$^-$ | MP4: dihydromyrcenol 0.74 MP5: geraniol 0.92; linalool oxide 0.84; $\alpha$-terpineol 0.81 |
| 39 | 1 | 4–5 | 7.78 | monoterpendiol-hexose-deoxyhexose $2^3$ ($C_{22}H_{38}O_{11}$) | 523.23900 478.24081 | 0.13 | | 477.23378 [M-H]$^-$ 163.06076 [Deoxyhexose-H]$^-$ | MP4: linalool oxide 0.72 MP5: geraniol 0.96; linalool oxide 0.88; $\alpha$-terpineol 0.87 |
| 40 | 1 | 4 | 7.80 | dehydromonoterpentriol-pentose-hexose-hexose 1 ($C_{27}H_{44}O_{17}$) | 639.25019 640.25747 | 0.25 | | 477.19656 [M-H-hexose+$H_2O$]$^-$ | MP1: $R^2 < 0.7$ MP4: linalool oxide 0.83 |
| 41 | 1 | 2–5 | 7.83 | norisoprenoid group G-hexose-hexose $1^3$ ($C_{25}H_{44}O_{13}$) | 551.27016 552.27744 | 0.38 | | 161.04440 [Hexose-H-$H_2O$]$^-$ | MP2: $R^2 < 0.7$ MP3: vitispiranes 0.93; Riesling acetal 0.92; TDN 0.82 MP4: $R^2 < 0.7$ MP5: TDN 0.95; Riesling acetal 0.95; vitispiranes 0.94; $\beta$-ionone 0.84 |
| 42 | 1 | 5 | 7.83 | dihydromonoterpenetraol-hexose-hexose 2 ($C_{22}H_{40}O_{14}$) | 527.23415 528.24142 | 0.31 | | 185.11752 [M-H-hexose-hexose+$H_2O$]$^-$ 179.05523 [Hexose-H]$^-$ | linalool oxide 0.94; geraniol 0.83; $\alpha$-terpineol 0.80 |
| 43 | 1 | 5 | 7.87 | ipsdienol-hexose-hexose-deoxypentose 3 ($C_{27}H_{44}O_{14}$) | 591.26522 592.27249 | 0.11 | | 429.21193 [M-H-hexose+$H_2O$]$^-$ | linalool oxide 0.93; geraniol 0.91; $\alpha$-terpineol 0.85 |
| 44 | 1 | 4–5 | 7.88 | citronellol/dihydromyrcenol-hexose-deoxypentose-pentose ($C_{26}H_{46}O_{13}$) | 565.28596 566.29324 | 0.11 | | 161.04507 [Hexose-H-$H_2O$]$^-$ 149.04531 [Pentose-H]$^-$ | MP4: $R^2 < 0.7$ MP5: geraniol 0.95; $\alpha$-terpineol 0.79; linalool oxide 0.77 |
| 45 | 1 | 4–5 | 7.90 | hydroxycitronellol-pentose-hexose $1^6$ ($C_{21}H_{40}O_{11}$) | 513.25466 468.25648 | 0.12 | | 467.24938 [M-H]$^-$ 333.19186 [M + HCOOH-H-hexose]$^-$ 335.20767 [Pentose-H + $H_2O$]$^-$ 161.04574 [Hexose-H-$H_2O$]$^-$ | MP4: $R^2 < 0.7$ MP5: geraniol 0.93; linalool oxide 0.90; $\alpha$-terpineol 0.84; dihydromyrcenol 0.70 |
| 46 | 1 | 4–5 | 7.93 | dihydromonoterpentriol-hexose-hexose 3 ($C_{22}H_{40}O_{13}$) | 511.23886 512.24613 | 0.41 | | 331.17617 [M-H-hexose]$^-$ 179.05527 [Hexose-H]$^-$ 161.04551 [Hexose-H-$H_2O$]$^-$ | MP4: linalool oxide 0.81 MP5: linalool oxide 0.87; $\alpha$-terpineol 0.78 |
| 47 | 1 | 1, 4–5 | 7.93 | geranic acid-hexose-hexose $1^6$ ($C_{22}H_{36}O_{12}$) | 537.21814 492.21996 | 0.36 | | 491.21312 [M-H]$^-$ 329.15993 [M-H-hexose+$H_2O$]$^-$ | MP1: $R^2 < 0.7$ MP4: dihydromyrcenol 0.70 MP5: geraniol 0.95; linalool oxide 0.90; $\alpha$-terpineol 0.87; dihydromyrcenol 0.72 |
| 48 | 1 | 4–5 | 7.99 | ipsdienol-deoxyhexose-pentose-pentose 2 ($C_{26}H_{42}O_{13}$) | 561.25456 562.26184 | 0.29 | | 163.0602 [Deoxyhexose-H]$^-$ 145.04970 [Deoxyhexose-H-$H_2O$]$^-$ | MP4: linalool oxide 0.77 MP5: geraniol 0.94; $\alpha$-terpineol 0.75 |

(*continued on next page*)

**Table 1** (*continued*)

| # | Cat[a] | MP[b] | $t_r^c$ (min) | Precursor and molecular formula | *m/z* exp[d] M exp[e] | Mass error[f] | Fragments MS-MS spectrum | | Coefficient of determination[g] |
|---|---|---|---|---|---|---|---|---|---|
| | | | | | | | Aglycone | Other fragments | |
| 49 | 1 | 5 | 8.02 | dihydromonoterpentriol-hexose-hexose 4 ($C_{22}H_{40}O_{13}$) | 511.23910 512.24638 | 0.06 | | 331.17600 [M-H-hexose]$^-$ 161.04580 [Hexose-H-$H_2O$]$^-$ | linalool oxide 0.92; geraniol 0.90; α-terpineol 0.82 |
| 50 | 1 | 4–5 | 8.03 | monoterpendiol-pentose-hexose $3^{3–11}$ ($C_{21}H_{36}O_{11}$) | 509.22332 464.22508 | 0.20 | | 463.21862 [M-H]$^-$, 331.17601 [M-H-pentose+$H_2O$]$^-$, 179.05601 [Hexose-H]$^-$, 161.04559 [Hexose-H-$H_2O$]$^-$ | MP4: $R^2 < 0.7$ MP5: geraniol 0.95; linalool oxide 0.85; α-terpineol 0.82 |
| 51 | 1 | 4–5 | 8.04 | geranic acid-hexose-pentose-pentose 1 ($C_{26}H_{42}O_{15}$) | 593.24425 594.25152 | 0.51 | | 413.17979 [M-H-hexose]$^-$ 131.03411 [Pentose-H-$H_2O$]$^-$ | MP4: $R^2 < 0.7$ MP5: linalool oxide 0.93; geraniol 0.90; α-terpineol 0.85 |
| 52 | 1 | 4–5 | 8.04 | hydroxycitronellol-hexose-deoxyhexose 2 ($C_{22}H_{42}O_{11}$) | 527.27011 482.27193 | 0.49 | | 481.26495 [M-H]$^-$ 335.20827 [M-H-deoxyhexose+H2O]- | MP4: $R^2 < 0.7$ MP5: geraniol 0.95; α-terpineol 0.80; linalool oxide 0.78 |
| 53 | 1 | 5 | 8.06 | monoterpenol-pentose-pentose-pentose ($C_{25}H_{42}O_{13}$) | 549.25451 550.26179 | 0.38 | | 149.04459 [Pentose-H]$^-$ | geraniol 0.95; linalool oxide 0.93; α-terpineol 0.87; dihydromyrcenol 0.74 |
| 54 | 1 | 4 | 8.07 | hydroxycitronellol-hexose-deoxyhexose-deoxyhexose ($C_{28}H_{52}O_{15}$) | 627.32201 628.32929 | 1.26 | | 447.25832 [M-H-hexose]$^-$ 463.25351 [M-H-deoxyhexose]$^-$ | α-terpineol 0.83 |
| 55 | 1 | 4 | 8.10 | 4-ethylguaiacol-pentose-deoxyhexose ($C_{20}H_{30}O_{10}$) | 475.18165 430.18346 | 0.20 | | 429.17619 [M-H]$^-$ 297.13354 [M-H-pentose-$H_2O$]$^-$ | guaiacol 0.80 |
| 56 | 1 | 4–5 | 8.13 | monoterpenol-pentose-deoxypentose-hexose ($C_{26}H_{44}O_{13}$) | 563.27028 564.27756 | 0.16 | | 161.04543 [Pentose-deoxypentose-H-$H_2O$]$^-$161.04542 [Hexose-H-$H_2O$]$^-$ | MP4: $R^2 < 0.7$ MP5: geraniol 0.92; α-terpineol 0.71 |
| 57 | 1 | 5 | 8.31 | monoterpenol-hexose-hexose-hexose ($C_{28}H_{48}O_{16}$) | 639.28605 640.29332 | 0.57 | | 459.22085 [M-H-hexose]$^-$ | geraniol 0.89; linalool oxide 0.86; α-terpineol 0.77 |
| 58 | 1 | 2–4 | 8.38 | norisoprenoid group G-hexose-hexose $2^3$ ($C_{25}H_{44}O_{13}$) | 551.27040 552.27768 | 0.05 | | 179.05496 [Hexose-H]$^-$ | MP 2: $R^2 < 0.7$ MP 3: vitispiranes 0.94; Riesling acetal 0.94; TDN 0.85 MP4 4: β-ionone 0.79 |
| 59 | 1 | 4 | 8.42 | norisoprenoid group F-hexose-hexose $1^3$ ($C_{25}H_{42}O_{13}$) | 549.25461 550.26188 | 0.20 | | 207.13802 [M-H-hexose-hexose]$^-$ | β-ionone 0.74 |
| 60 | 1 | 5 | 8.45 | citronellol/dihydromyrcenol-deoxyhexose-hexose-pentose 1 ($C_{27}H_{48}O_{14}$) | 595.29675 596.30402 | 0.28 | | 161.04546 [Hexose-H-$H_2O$]$^-$ | linalool oxide 0.92; geraniol 0.92; α-terpineol 0.87 |
| 61 | 1 | 4 | 8.46 | monoterpenol-deoxypentose-deoxyhexose-hexose 1 ($C_{27}H_{46}O_{13}$) | 577.28588 578.29315 | 0.24 | | 397.22278 [M-H-hexose]$^-$ | linalool oxide 0.74 |
| 62 | 1 | 4–5 | 8.51 | citronellol/dihydromyrcenol-hexose-deoxyhexose 1 ($C_{22}H_{40}O_{10}$) | 463.25425 464.26153 | 0.24 | | 301.20191 [M-H-hexose+$H_2O$]$^-$ 299.18556 [M-H-deoxyhexose]$^-$ 283.03399 [M-H-hexose]$^-$ | MP4: linalool oxide 0.70 MP5: geraniol 0.94; linalool oxide 0.87; α-terpineol 0.83; dihydromyrcenol 0.70 |
| 63 | 1 | 4–5 | 8.61 | dihydromonoterpenetraol-pentose-pentose-hexose ($C_{26}H_{46}O_{17}$) | 629.26512 630.27239 | 0.89 | | 161.04527 [Hexose-H-$H_2O$]$^-$ | MP4: α-terpineol 0.92 MP5: linalool oxide 0.96; geraniol 0.89; α-terpineol 0.86 |
| 64 | 1 | 4–5 | 8.84 | monoterpenol-pentose-hexose$^{3–11}$ ($C_{21}H_{36}O_{10}$) | 493.22863 448.23059 | 0.25 | | 447.22333 [M-H]$^-$ 315.18022 [M-H-pentose+$H_2O$]$^-$ 161.04527 [Hexose-H-$H_2O$]$^-$ | MP4: $R^2 < 0.7$ MP5: α-terpineol 0.94; linalool oxide 0.94; geraniol 0.81 |
| 65 | 1 | 5 | 8.92 | geranic acid-hexose-hexose $2^6$ ($C_{22}H_{36}O_{12}$) | 491.21289 492.22017 | 0.07 | | 161.04534 [Hexose-H-$H_2O$]$^-$ | linalool oxide 0.94; α-terpineol 0.78; geraniol 0.75 |
| 66 | 1 | 5 | 8.97 | monoterpenol-deoxypentose-deoxyhexose-hexose 2 ($C_{27}H_{46}O_{13}$) | 577.28589 578.29316 | 0.23 | | 397.22256 [M-H-hexose]$^-$ 161.04492 [Hexose-H-$H_2O$]$^-$ | linalool oxide 0.95; geraniol 0.84; α-terpineol 0.83 |
| 67 | 1 | 4 | 9.00 | norisoprenoid group E-hexose-hexose 2 ($C_{25}H_{40}O_{13}$) | 547.23923 548.24651 | 0.29 | | 161.04534 [Hexose-H-$H_2O$]$^-$ | β-ionone 0.73 |

(*continued on next page*)

**Table 1** (*continued*)

| # | Cat[a] | MP[b] | $t_r^c$ (min) | Precursor and molecular formula | *m/z* exp[d] M exp[e] | Mass error[f] | Fragments MS-MS spectrum | | Coefficient of determination[g] |
|---|---|---|---|---|---|---|---|---|---|
| | | | | | | | Aglycone | Other fragments | |
| 68 | 1 | 4–5 | 9.07 | monoterpenol-pentose-deoxyhexose-deoxyhexose ($C_{27}H_{46}O_{13}$) | 577.28588 578.29316 | 0.24 | | 149.04501 [Pentose-H]$^-$ | MP4: $R^2 < 0.7$ MP5: geraniol 0.93; linalool oxide 0.92; $\alpha$-terpineol 0.85; dihydromyrcenol 0.70 |
| 69 | 1 | 4–5 | 9.20 | dehydromonoterpentriol-pentose-hexose-hexose 2 ($C_{27}H_{44}O_{17}$) | 639.25025 640.25753 | 0.34 | | 149.04541 [Pentose-H]$^-$ 323.09782 [Hexose-hexose-H-$H_2O$]$^-$ | MP4: geraniol 0.93; linalool oxide 0.89; $\alpha$-terpineol 0.84 MP5: linalool oxide 0.86 |
| 70 | 1 | 1–4 | 9.23 | norisoprenoid group C-deoxypentose-hexose ($C_{24}H_{42}O_{10}$) | 489.27003 490.27731 | 0.11 | | 327.21769 [M-H-hexose+$H_2O$]$^-$ 309.20809 [M-H-hexose]$^-$ | MP1: $\beta$-damascenone 0.88 MP2: $\beta$-damascenone 0.87 MP3: Riesling acetal 0.77; $\alpha$-ionone 0.74 MP4: $\beta$-ionone 0.81 |
| 71 | 1 | 4–5 | 9.26 | geranic acid-pentose-hexose[6,10] ($C_{21}H_{34}O_{11}$) | 507.20773 462.20958 | 0.08 | 167.10750 | 461.20228 [M-H]$^-$ 149.04454 [Pentose-H]$^-$ | MP4: $R^2 < 0.7$ MP5: geraniol 0.89; linalool oxide 0.88; $\alpha$-terpineol 0.81 |
| 72 | 1 | 4–5 | 9.27 | monoterpendiol-hexose-hexose 1[10] ($C_{22}H_{38}O_{12}$) | 493.22863 494.23591 | 0.25 | | 161.04527 [Hexose-H-$H_2O$]$^-$ | MP4: $R^2 < 0.7$ MP5: linalool oxide 0.96; geraniol 0.86; $\alpha$-terpineol 0.86 |
| 73 | 1 | 4 | 9.67 | hydroxycitronellol-pentose-pentose ($C_{20}H_{38}O_{10}$) | 483.24410 438.24563 | 0.11 | | 437.24061 [M-H]$^-$ 131.03507 [Pentose-H-$H_2O$]$^-$ | dihydromyrcenol 0.77; geraniol 0.76; linalool 0.75 |
| 74 | 1 | 4–5 | 9.88 | hydroxycitronellol-deoxyhexose-pentose-pentose 1 ($C_{26}H_{48}O_{14}$) | 583.29650 584.30377 | 0.15 | | 301.20249 [M-H-pentose-pentose]$^-$ | MP4: linalool oxide 0.82 MP5: geraniol 0.92; linalool oxide 0.87; $\alpha$-terpineol 0.83 |
| 75 | 1 | 4 | 10.04 | hydroxycitronellol-deoxyhexose-pentose-pentose 2 ($C_{26}H_{48}O_{14}$) | 583.29652 584.30379 | 0.11 | | 301.20249 [M-H-pentose-pentose]$^-$ | linalool oxide 0.77 |
| 76 | 2 | 4 | 4.95 | acetovanillone-hexose 1[1,8,12] ($C_{15}H_{20}O_8$) | 373.11375 328.11557 | 0.74 | | 327.10774 [M-H]$^-$ 193.05096 [M + HCOOH-H-hexose]$^-$ | |
| 77 | 2 | 4–5 | 5.65 | furaneol-pentose-hexose[6] ($C_{17}H_{26}O_{12}$) | 467.14048 422.14229 | 0.85 | | 421.13386 [M-H]$^-$ 289.09103 [M-H-pentose+$H_2O$]$^-$ | |
| 78 | 2 | 5 | 5.65 | furaneol-pentose-pentose-hexose ($C_{22}H_{34}O_{16}$) | 553.17727 554.18454 | 0.73 | | 179.05623 [Hexose-H]$^-$ | |
| 79 | 2 | 4–5 | 5.72 | acetovanillone-hexose 2[1,8,12] ($C_{15}H_{20}O_8$) | 373.11395 328.11577 | 1.27 | | 327.10794 [M-H]$^-$ 193.05083 [M + HCOOH-H-hexose]$^-$ 179.05558 [Hexose-H]$^-$ | |
| 80 | 2 | 1,4 | 5.82 | ethoxymethylmethoxyphenol-hexose-hexose-deoxyhexose 1 ($C_{28}H_{44}O_{17}$) | 651.25001 652.25729 | 0.03 | | 161.04515 [Hexose-H-$H_2O$]$^-$ | |
| 81 | 2 | 1, 4–5 | 5.83 | vanillin-hexose 1[1,7,12] ($C_{14}H_{18}O_8$) | 359.09830 314.10011 | 1.32 | 197.04571 [Aglycone+HCOOH]$^-$ | 313.09282 [M-H]$^-$ | |
| 82 | 2 | 4 | 5.94 | syringaldehyde-hexose-hexose 1[1,12] ($C_{21}H_{30}O_{14}$) | 505.15594 506.16272 | 0.41 | 181.05118 | 343.10457 [M-H-hexose+$H_2O$]$^-$ | |
| 83 | 2 | 4–5 | 6.03 | acetovanillone-hexose-hexose ($C_{21}H_{30}O_{13}$) | 535.16508 490.16690 | 2.28 | 165.05486 | 489.15907 [M-H]$^-$ 327.10809 [M-H-hexose+$H_2O$]$^-$ | |
| 84 | 2 | 4 | 6.10 | vanillin-hexose-hexose 1[1] ($C_{20}H_{28}O_{13}$) | 521.15033 476.15267 | 0.61 | | 475.14484 [M-H]$^-$ 323.07775 [M + HCOOH-H-$H_2O$-hexose]$^-$161.02421 [M + HCOOH-H-$H_2O$-hexose-hexose]$^-$ | |
| 85 | 2 | 4–5 | 6.15 | syringaldehyde-hexose 1[1,8,12] ($C_{15}H_{20}O_9$) | 343.10350 344.11077 | 1.72 | 181.05131 | | |
| 86 | 2 | 4–5 | 6.15 | syringaldehyde-hexose-hexose 2[1,12] ($C_{21}H_{30}O_{14}$) | 551.16177 506.16359 | 1.01 | 181.05101 | 505.15576 [M-H]$^-$ 343.10285 [M-H-hexose]$^-$ | |
| 87 | 2 | 1, 4–5 | 6.16 | furaneol-pentose-pentose ($C_{16}H_{24}O_{11}$) | 437.1296 392.13142 | 0.18 | | 391.12414 [M-H]$^-$ 259.08220 [M-H-pentose+$H_2O$]$^-$ | |

(*continued on next page*)

**Table 1** (*continued*)

| # | Cat[a] | MP[b] | $t_r^c$ (min) | Precursor and molecular formula | *m/z* exp[d] M exp[e] | Mass error[f] | Fragments MS-MS spectrum | | Coefficient of determination[g] |
|---|---|---|---|---|---|---|---|---|---|
| | | | | | | | Aglycone | Other fragments | |
| 88 | 2 | 1 | 6.28 | vanillin-hexose 2[1,7,12] ($C_{14}H_{18}O_8$) | 359.09798<br>314.09980 | 0.43 | 197.04435 [Aglycone+HCOOH]$^-$ | 313.09197 [M-H]$^-$ | |
| 89 | 2 | 4,5 | 6.38 | ethoxymethylmethoxyphenol-hexose-hexose-deoxyhexose 2 ($C_{28}H_{44}O_{17}$) | 651.24984<br>652.25712 | 0.29 | | 179.05590 [Hexose-H]$^-$<br>161.04458 [Hexose-H-$H_2O$]$^-$ | |
| 90 | 2 | 1, 4–5 | 6.40 | acetovanillone-hexose 3[1,8,12] ($C_{15}H_{20}O_8$) | 373.11451<br>328.11633 | 2.77 | 165.05627<br>211.06188<br>[Aglycone+HCOOH]$^-$ | 327.10850 [M-H]$^-$ | |
| 91 | 2 | 5 | 6.41 | furaneol-hexose-deoxyhexose ($C_{18}H_{28}O_{12}$) | 435.15059<br>436.15786 | 0.77 | | 109.02982 [M-H-hexose-deoxyhexose]$^-$ | |
| 92 | 2 | 1, 5 | 6.41 | syringaldehyde-hexose 2[1,8,12] ($C_{15}H_{20}O_9$) | 343.10331<br>344.11059 | 1.17 | 181.05076 | | |
| 93 | 2 | 4–5 | 6.44 | vanillin-hexose 3[1,7,12] ($C_{14}H_{18}O_8$) | 313.09264<br>314.09991 | 0.94 | 151.04022 | | |
| 94 | 2 | 1, 4 | 6.50 | vanillin-pentose-hexose[1] ($C_{19}H_{26}O_{12}$) | 491.14054<br>446.14235 | 0.93 | 197.04468 [Aglycone+HCOOH]$^-$ | 445.13452 [M-H]$^-$. 311.07695 [M + HCOOH-H-hexose]$^-$. 161.04507 [Hexose-H-$H_2O$]$^-$. 131.03486 [Pentose-H-$H_2O$]$^-$ | |
| 95 | 2 | 4 | 6.57 | vanillin-hexose-hexose 2[1] ($C_{20}H_{28}O_{13}$) | 521.15094<br>476.15275 | 0.56 | 197.04471 [Aglycone+HCOOH]$^-$ | 475.14492 [M-H]$^-$<br>341.08897 [M + HCOOH-H-hexose]$^-$ | |
| 96 | 2 | 4–5 | 6.61 | ethyl leucate-hexose-pentose-pentose 1 ($C_{24}H_{42}O_{16}$) | 631.24509<br>586.24691 | 0.23 | | 585.23908 [M-H]$^-$, 423.18738 [M-H-hexose+$H_2O$]$^-$, 405.17753 [M-H-hexose]$^-$, 303.1461 [M-H-pentose-pentose]$^-$ | |
| 97 | 2 | 1, 4 | 6.61 | syringaldehyde-hexose 3 [1,8,12] ($C_{15}H_{20}O_9$) | 343.10320<br>344.11048 | 0.85 | 181.05056 | | |
| 98 | 2 | 5 | 6.62 | vanillin-pentose[1,12] ($C_{13}H_{16}O_7$) | 329.08790<br>284.08971 | 1.94 | | 283.08188 [M-H]$^-$<br>179.03484 [M + HCOOH-H-pentose]$^-$ | |
| 99 | 2 | 1, 4 | 6.64 | coniferaldehyde-deoxyhexose-deoxypentose ($C_{21}H_{28}O_{10}$) | 439.16087<br>440.16815 | 1.01 | 195.06666 [Aglycone+$H_2O$]$^-$ | | |
| 100 | 2 | 4–5 | 6.65 | ethyl leucate-hexose ($C_{14}H_{26}O_8$) | 367.16019<br>322.16253 | 0.64 | | 321.1547 [M-H]$^-$<br>161.04542 [Hexose-H-$H_2O$]$^-$ | |
| 101 | 2 | 1, 4 | 6.65 | sinapaldehyde-deoxyhexose-deoxypentose ($C_{22}H_{30}O_{11}$) | 469.17182<br>470.17910 | 1.77 | 225.07596 [Aglycone+$H_2O$]$^-$ | | |
| 102 | 2 | 4–5 | 6.83 | ethyl leucate-hexose-pentose-pentose 2 ($C_{24}H_{42}O_{16}$) | 585.23936<br>586.24663 | 0.18 | | 423.18814 [M-H-hexose+$H_2O$]$^-$<br>179.05638 [Hexose-H]$^-$ | |
| 103 | 2 | 4 | 6.95 | vanillin-hexose-hexose 3[1] ($C_{20}H_{28}O_{13}$) | 521.15104<br>476.15285 | 0.75 | 151.03981 | 475.14502 [M-H]- | |
| 104 | 2 | 4 | 7.06 | ethyl leucate-hexose-pentose-pentose 3 ($C_{24}H_{42}O_{16}$) | 585.23939<br>586.24667 | 0.13 | | 423.18617 [M-H-hexose-$H_2O$]$^-$<br>405.17715 [M-H-hexose]$^-$ | |
| 105 | 2 | 1, 4 | 7.07 | etoximetilmetoxifenol-hexose[1,8,12] ($C_{16}H_{24}O_8$) | 343.13954<br>344.14681 | 0.71 | 181.08673 | | |
| 106 | 2 | 4–5 | 7.10 | vanillin-hexose 4[1,7,12] ($C_{14}H_{18}O_8$) | 359.09767<br>314.09948 | 0.43 | 197.04393 [Aglycone+HCOOH]$^-$ | 313.09165 [M-H]$^-$ | |
| 107 | 2 | 4 | 7.24 | syringaldehyde-hexose 4[1,8,12] ($C_{15}H_{20}O_9$) | 343.10286<br>344.11014 | 0.15 | 181.05022 | | |
| 108 | 2 | 4 | 7.28 | ethyl leucate-hexose-pentose-pentose 4 ($C_{24}H_{42}O_{16}$) | 631.24474<br>586.24656 | 0.32 | | 585.23873 [M-H]$^-$,<br>179.05603 [Hexose-H]$^-$,<br>149.04511 [Pentose-H]$^-$ | |
| 109 | 2 | 5 | 7.98 | eugenol/isoeugenol-hexose-deoxyhexose[13] ($C_{22}H_{32}O_{11}$) | 471.18725<br>472.19452 | 1.29 | 163.07587 | | |
| 110 | 2 | 1, 4 | 7.98 | eugenol/isoeugenol-pentose-deoxyhexose-deoxyhexose 1 ($C_{27}H_{40}O_{14}$) | 587.23388<br>588.24116 | 0.18 | | 149.04536 [Pentose-H]$^-$ | |
| 111 | 2 | 1,4 | 8.08 | sinapaldehyde-deoxyhexose 1 ($C_{17}H_{22}O_8$) | 353.12424<br>354.13152 | 1.68 | | 145.04998 [Deoxyhexose-H-$H_2O$]$^-$ | |
| 112 | 2 | 4–5 | 8.09 | eugenol/isoeugenol-pentose-deoxyhexose-deoxyhexose 2 ($C_{27}H_{40}O_{14}$) | 587.23398<br>588.24126 | 0.01 | | 149.04566 [Pentose-H]$^-$<br>131.03396 [Pentose-H-$H_2O$]$^-$ | |
| 113 | 2 | 1, 4 | 8.24 | eugenol/isoeugenol-pentose-hexose[13] ($C_{21}H_{30}O_{11}$) | 503.17644<br>458.17826 | 0.06 | 209.08167 [Aglycone+HCOOH]$^-$ | 457.17043 [M-H]$^-$ | |

(*continued on next page*)

**Table 1** (*continued*)

| # | Cat[a] | MP[b] | $t_r^c$ (min) | Precursor and molecular formula | *m/z* exp[d] M exp[e] | Mass error[f] | Fragments MS-MS spectrum | | Coefficient of determination[g] |
|---|---|---|---|---|---|---|---|---|---|
| | | | | | | | Aglycone | Other fragments | |
| 114 | 2 | 4–5 | 8.26 | ethoxymethylmethoxyphenol-deoxyhexose-deoxyhexose-deoxypentose ($C_{27}H_{42}O_{14}$) | 589.24879<br>590.25607 | 1.43 | 181.08627 | | |
| 115 | 2 | 4 | 8.39 | sinapaldehyde-deoxyhexose 2 ($C_{17}H_{22}O_8$) | 353.12424<br>354.13152 | 1.68 | | 145.04957 [Deoxyhexose-H-$H_2O$]$^-$ | |
| 116 | 2 | 1 | 8.60 | eugenol/isoeugenol-pentose-deoxyhexose-deoxyhexose 3 ($C_{27}H_{40}O_{14}$) | 587.23422<br>588.24150 | 0.40 | | 131.03468 [Pentose-H-$H_2O$]$^-$ | |
| 117 | 2 | 1, 4 | 8.77 | ethyl leucate-hexose-deoxyhexose ($C_{20}H_{36}O_{12}$) | 467.21279<br>468.22006 | 0.14 | | 161.04528 [Hexose-H-$H_2O$]$^-$ | |
| 118 | 3 | 4–5 | 5.59 | syringol-hexose[1–2,8,12–13] ($C_{14}H_{20}O_8$) | 315.10849<br>316.11576 | 1.57 | 153.05579 | | MP4: $R^2 < 0.7$<br>MP5: < DL |
| 119 | 3 | 4 | 5.74 | monohydroxycinnamic acid-hexose-hexose 1[1,8,12] ($C_{21}H_{28}O_{13}$) | 533.15087<br>488.15268 | 0.41 | 163.04034 | 487.14541 [M-H]$^-$<br>325.09219 [M-H-hexose+$H_2O$]$^-$<br>477.16133 [M-H]$^-$ | < DL |
| 120 | 3 | 5 | 5.75 | syringol-hexose-hexose 1[1,12–13] ($C_{20}H_{30}O_{13}$) | 523.16699<br>478.16880 | 1.32 | 153.0556 | 315.10752 [M + HCOOH-H-hexose]$^-$<br>135.0448 [M-HCOOH-H-hexose-hexose]$^-$ | < DL |
| 121 | 3 | 5 | 5.90 | monohydroxymethoxycinnamic acid-hexose-pentose 1[1,8,12] ($C_{21}H_{28}O_{13}$) | 487.14578<br>488.15306 | 1.25 | 193.05010 | 325.09213 [M-H]- | < DL |
| 122 | 3 | 4–5 | 5.93 | monohydroxymethoxycinnamic acid-hexose-hexose[12] ($C_{22}H_{30}O_{14}$) | 563.16140<br>518.16322 | 0.33 | 193.05101 | 517.15623 [M-H]$^-$ | MP4: < DL<br>MP5: < DL |
| 123 | 3 | 1 | 5.97 | dihydroxycinnamic acid-hexose 1[1,8,12] ($C_{15}H_{18}O_9$) | 341.08765<br>342.09492 | 1.14 | 179.03370 | 161.02361 [M-H-hexose]$^-$ | $R^2 < 0.7$ |
| 124 | 3 | 1, 4–5 | 6.00 | monohydroxycinnamic acid-hexose 1[1,8,12] ($C_{15}H_{18}O_8$) | 371.09860<br>326.10041 | 2.09 | 163.04018 | 325.09288 [M-H]$^-$ | MP 1: $R^2 < 0.7$<br>MP4: < DL<br>MP5: < DL |
| 125 | 3 | 1, 5 | 6.00 | monohydroxycinnamic acid-hexose-hexose 2[1,8,12] ($C_{21}H_{28}O_{13}$) | 533.15051<br>488.15232 | 0.26 | 163.04019 | 487.14505 [M-H]$^-$<br>325.09349 [M-H-hexose+$H_2O$]$^-$ | MP 1: $R^2 < 0.7$<br>MP 5: < DL |
| 126 | 3 | 1 | 6.17 | dihydroxycinnamic acid-hexose 2[1,8,12] ($C_{15}H_{18}O_9$) | 341.08764<br>342.09492 | 1.11 | 179.03387 | 161.02414 [M-H-hexose]$^-$ | $R^2 < 0.7$ |
| 127 | 3 | 4–5 | 6.18 | syringol-hexose-deoxyhexose 1[13] ($C_{20}H_{30}O_{12}$) | 461.16624<br>462.17330 | 0.73 | 153.05541 | | MP4: $R^2 < 0.7$<br>MP5: < DL |
| 128 | 3 | 5 | 6.23 | dihydromonoterpentriol-hexose-pentose-pentose ($C_{26}H_{46}O_{16}$) | 613.27109<br>614.27837 | 0.53 | | 179.05585 [Hexose-H]$^-$ | $R^2 < 0.7$ |
| 129 | 3 | 4 | 6.24 | ipsdienol-hexose-hexose-hexose ($C_{28}H_{46}O_{16}$) | 683.27636<br>638.27818 | 0.17 | | 637.27090 [M-H]$^-$<br>179.05521 [Hexose-H]$^-$ | $R^2 < 0.7$ |
| 130 | 3 | 5 | 6.31 | syringol-hexose-hexose 2[1,12–13] ($C_{20}H_{30}O_{13}$) | 477.16131<br>478.16858 | 1.03 | | 161.04478 [Hexose-H-$H_2O$]$^-$ | < DL |
| 131 | 3 | 5 | 6.32 | monohydroxymethoxycinnamic acid-hexose 1[1,8,12] ($C_{16}H_{20}O_9$) | 355.10398<br>356.11126 | 3.01 | 193.05188 | | < DL |
| 132 | 3 | 4–5 | 6.33 | dihydroxycinnamic acid-hexose 3[1,8,12] ($C_{15}H_{18}O_9$) | 341.08770<br>342.09498 | 1.29 | 179.03533 | 179.05553 [Hexose-H]$^-$<br>161.02457 [M-H-hexose]$^-$ | MP4: < DL<br>MP5: < DL |
| 133 | 3 | 4 | 6.33 | syringol-hexose-deoxyhexose 2[13] ($C_{20}H_{30}O_{12}$) | 461.16633<br>462.17361 | 0.92 | 153.05533 | | $R^2 < 0.7$ |
| 134 | 3 | 5 | 6.35 | monoterpendiol-hexose-pentose-pentose 2 ($C_{26}H_{44}O_{15}$) | 595.26023<br>596.26751 | 0.05 | | 161.04571 [Hexose-H-$H_2O$]$^-$<br>149.04534 [Pentose-H]$^-$<br>131.03489 [Pentose-H-$H_2O$]$^-$ | $R^2 < 0.7$ |
| 135 | 3 | 3 | 6.36 | 4-ethylphenol-hexose-hexose[1,10] ($C_{20}H_{30}O_{11}$) | 491.17716<br>446.17898 | 1.40 | 121.06517 | 445.17115 [M-H]$^-$ | $R^2 < 0.7$ |
| 136 | 3 | 1, 4–5 | 6.38 | dihydroxycinnamic acid-hexose-hexose 1[1,12] ($C_{21}H_{28}O_{14}$) | 503.14043<br>504.14770 | 0.69 | 179.03488 | 323.0768 [M-H-hexose]-<br>161.02407 [M-H-hexose-hexose]- | MP1: $R^2 < 0.7$<br>MP4: < DL<br>MP5: < DL |
| 137 | 3 | 4–5 | 6.50 | 4-ethylguaiacol-pentose-deoxyhexose-deoxyhexose ($C_{26}H_{40}O_{14}$) | 575.23334<br>576.24062 | 1.12 | | 443.19238 [M-H-Pentose+$H_2O$]$^-$<br>131.03435 [Pentose-H-$H_2O$]$^-$ | MP4: $R^2 < 0.7$<br>MP5: < DL |
| 138 | 3 | 4 | 6.52 | 4-ethylphenol-hexose[1] ($C_{14}H_{20}O_6$) | 329.12418<br>284.12600 | 1.63 | 167.07200 [Aglycone+HCOOH]$^-$ | 283.11817 [M-H]$^-$ | $R^2 < 0.7$ |
| 139 | 3 | 1, 4 | 6.54 | dihydroxycinnamic acid-hexose 4[1,8,12] ($C_{15}H_{18}O_9$) | 341.08769<br>342.09497 | 1.26 | 179.03506 | | MP1: $R^2 < 0.7$<br>MP4: < DL |

(*continued on next page*)

**Table 1** (*continued*)

| # | Cat[a] | MP[b] | $t_r^c$ (min) | Precursor and molecular formula | *m/z* exp[d] M exp[e] | Mass error[f] | Fragments MS-MS spectrum | | Coefficient of determination[g] |
|---|---|---|---|---|---|---|---|---|---|
| | | | | | | | Aglycone | Other fragments | |
| 140 | 3 | 5 | 6.61 | norisoprenoid group F-hexose-hexose 2[3] ($C_{25}H_{42}O_{13}$) | 595.26061<br>550.26239 | 0.69 | | 549.25456 $[M-H]^-$<br>179.05618 $[Hexose-H]^-$ | $R^2 < 0.7$ |
| 141 | 3 | 4 | 6.63 | dihydroxycinnamic acid-hexose-hexose 2[1,12] ($C_{21}H_{28}O_{14}$) | 503.14048<br>504.14776 | 0.79 | 179.03541 | 161.02506 [M-H-hexose-hexose]- | < DL |
| 142 | 3 | 5 | 6.64 | cresol-hexose-hexose ($C_{19}H_{28}O_{11}$) | 477.16112<br>432.16289 | 0.63 | 153.05503 $[Aglycone+HCOOH]^-$ | 431.15506 $[M-H]^-$<br>161.04563 $[Hexose-H-H_2O]^-$ | < DL |
| 143 | 3 | 4 | 6.66 | syringol-deoxyhexose ($C_{14}H_{20}O_7$) | 345.11854<br>300.12036 | 0.06 | | 299.11253 $[M-H]^-$<br>181.05044 $[M + HCOOH-H-deoxyhexose]^-$ | $R^2 < 0.7$ |
| 144 | 3 | 5 | 6.67 | cresol-hexose-pentose-pentose[2] ($C_{23}H_{34}O_{14}$) | 579.19284<br>534.19487 | 0.56 | | 533.18704 $[M-H]^-$<br>269.10369 $[M-H-pentose-pentose+H_2O]^-$ | < DL |
| 145 | 3 | 4 | 6.69 | dihydroxycinnamic acid-hexose 5[1,8,12] ($C_{15}H_{18}O_9$) | 341.08756<br>342.09484 | 0.88 | 179.03497 | 161.02481 $[M-H-hexose]^-$ | < DL |
| 146 | 3 | 4 | 6.75 | monohydroxycinnamic acid-hexose 2[1,8,12] ($C_{15}H_{18}O_8$) | 325.09290<br>326.10018 | 1.71 | 163.03947 | 145.02934 $[M-H-hexose]^-$ | < DL |
| 147 | 3 | 5 | 6.78 | monohydroxymethoxycinnamic acid-hexose-pentose 2[1,8,12] ($C_{21}H_{28}O_{13}$) | 487.14560<br>488.15305 | 0.88 | | 307.08287 $[M-H-hexose]^-$<br>161.04436 $[Hexose-H-H_2O]^-$ | < DL |
| 148 | 3 | 4 | 6.98 | dihydromonoterpenetraol-hexose-hexose 3 ($C_{22}H_{40}O_{14}$) | 527.23388<br>528.24116 | 0.20 | | 347.17176 $[M-H-hexose]^-$ | $R^2 < 0.7$ |
| 149 | 3 | 4 | 6.99 | monohydroxymethoxycinnamic acid-hexose 2[1,8,12] ($C_{16}H_{20}O_9$) | 355.10346<br>356.11074 | 1.55 | 193.05013 | 175.04013 $[M-H-hexose]^-$ | < DL |
| 150 | 3 | 4 | 7.02 | monohydroxycinnamic acid-hexose 3[1,8,12] ($C_{15}H_{18}O_8$) | 325.09275<br>326.10002 | 1.25 | 163.03960 | 145.02934 $[M-H-hexose]^-$ | < DL |
| 151 | 3 | 1 | 7.04 | dihydroxycinnamic acid-hexose 6[1,8,12] ($C_{15}H_{18}O_9$) | 341.08745<br>342.09473 | 0.56 | 179.03436 | | $R^2 < 0.7$ |
| 152 | 3 | 4–5 | 7.05 | cresol-pentose-hexose[1–4,6,8,10] ($C_{18}H_{26}O_{10}$) | 447.15047<br>402.15224 | 0.48 | | 401.14441 $[M-H]^-$<br>131.03503 $[Pentose-H-H_2O]^-$ | MP4: < DL<br>MP5: < DL |
| 153 | 3 | 4 | 7.12 | norisoprenoid group F-pentose-hexose 4 ($C_{24}H_{40}O_{12}$) | 565.24835<br>520.25009 | 2.27 | | 519.24226 $[M-H]^-$<br>385.18646 $[M + HCOOH-H-hexose]^-$<br>293.0873 $[Pentose-hexose-H-H_2O]^-$ | $R^2 < 0.7$ |
| 154 | 3 | 5 | 7.14 | cresol-hexose-hexose-hexose ($C_{25}H_{38}O_{16}$) | 593.20839<br>594.21567 | 0.38 | | 323.09785 $[Hexose-hexose-H_2O]^-$<br>179.05576 $[Hexose-H]^-$ | < DL |
| 155 | 3 | 5 | 7.14 | monoterpendiol-hexose-pentose-pentose 3 ($C_{26}H_{44}O_{15}$) | 595.26023<br>596.26751 | 0.05 | | 179.05528 $[Hexose-H]^-$,<br>161.04534 $[Hexose-H-H_2O]^-$, 149.04442 $[Pentose-H]^-$ | $R^2 < 0.7$ |
| 156 | 3 | 4 | 7.20 | ipsdienol-pentose-pentose-hexose ($C_{26}H_{42}O_{14}$) | 577.24975<br>578.25703 | 0.20 | | 161.04456 $[Hexose-H-H_2O]^-$<br>131.03494 $[Pentose-H-H_2O]^-$ | $R^2 < 0.7$ |
| 157 | 3 | 4, 5 | 7.20 | cresol-hexose-deoxyhexose[2] ($C_{19}H_{28}O_{10}$) | 461.16596<br>416.16779 | 0.12 | | 415.15996 $[M-H]^-$<br>161.04511 $[Hexose-H-H_2O]^-$ | MP 4: < DL<br>MP 5: < DL |
| 158 | 3 | 4 | 7.25 | monoterpendiol-pentose-pentose ($C_{20}H_{34}O_{10}$) | 479.21228<br>434.21462 | 1.20 | | 433.20679 $[M-H]^-$,<br>149.04539 $[Pentose-H]^-$,<br>131.03497 $[Pentose-H-H_2O]^-$ | $R^2 < 0.7$ |
| 159 | 3 | 4 | 7.33 | monoterpendiol-pentose-hexose 4[3–11] ($C_{21}H_{36}O_{11}$) | 509.22356<br>464.22538 | 0.27 | | 463.21755 $[M-H]^-$,<br>331.17585 $[M-H-pentose+H_2O]^-$,179.05488 $[Hexose-H]^-$, 161.04484 $[Hexose-H-H_2O]^-$ | $R^2 < 0.7$ |
| 160 | 3 | 5 | 7.39 | 4-ethylphenol-hexose-hexose-pentose ($C_{25}H_{38}O_{15}$) | 623.21866<br>578.22047 | 0.11 | | 577.21264 $[M-H]^-$,<br>161.04464 $[Hexose-H-H_2O]^-$,<br>131.03445 $[Pentose-H-H_2O]^-$ | < DL |
| 161 | 3 | 4 | 7.42 | syringol-hexose-deoxyhexose 3[13] ($C_{20}H_{30}O_{12}$) | 461.16614<br>462.17341 | 0.51 | | 161.04547 $[Hexose-H-H_2O]^-$ | $R^2 < 0.7$ |
| 162 | 3 | 4 | 7.49 | monoterpendiol-pentose-hexose 5[3–11] ($C_{21}H_{36}O_{11}$) | 509.22347<br>464.22528 | 0.10 | | 463.21745 $[M-H]^-$,<br>331.17421 $[Pentose-H + H_2O]^-$,<br>179.05512 $[Hexose-H]^-$,<br>149.04557 $[Pentose-H]^-$ | $R^2 < 0.7$ |
| 163 | 3 | 4–5 | 7.55 | syringol-hexose-deoxyhexose 4[13] ($C_{20}H_{30}O_{12}$) | 461.16600<br>462.17328 | 0.21 | | 161.04553 $[Hexose-H-H_2O]^-$ | MP4: $R^2 < 0.7$<br>MP5: < DL |

(*continued on next page*)

**Table 1** (*continued*)

| # | Cat[a] | MP[b] | $t_r^c$ (min) | Precursor and molecular formula | *m/z* exp[d] M exp[e] | Mass error[f] | Fragments MS-MS spectrum | | Coefficient of determination[g] |
|---|---|---|---|---|---|---|---|---|---|
| | | | | | | | Aglycone | Other fragments | |
| 164 | 3 | 1, 4–5 | 7.58 | dehydromonoterpentriol-hexose[3–5] ($C_{16}H_{26}O_8$) | 391.16083 346.16265 | 1.04 | 183.10177 | 345.15459 $[M-H]^-$ | MP1: $R^2 < 0.7$ MP4: $R^2 < 0.7$ MP5: $R^2 < 0.7$ |
| 165 | 3 | 4 | 7.60 | ipsdienol-pentose-hexose 1 ($C_{21}H_{34}O_{10}$) | 445.20758 446.21486 | 0.46 | | 161.04405 $[Hexose-H-H_2O]^-$ | $R^2 < 0.7$ |
| 166 | 3 | 4 | 7.72 | monoterpendiol-pentose-hexose 6[3–11] ($C_{21}H_{36}O_{11}$) | 509.22347 464.22526 | 0.10 | | 463.21743 $[M-H]^-$, 331.17547 $[M-H-pentose+H_2O]^-$, 179.05476 $[Hexose-H]^-$, 161.04534 $[Hexose-H-H_2O]^-$ | $R^2 < 0.7$ |
| 167 | 3 | 5 | 7.84 | hydroxycitronellol-deoxyhexose-deoxyhexose-deoxyhexose ($C_{28}H_{52}O_{14}$) | 657.33334 612.33515 | 0.04 | | 611.32675 $[M-H]^-$ 465.26911 $[M-H-deoxyhexose+H_2O]^-$ 665.30103 $[M-H]^-$ | $R^2 < 0.7$ |
| 168 | 3 | 5 | 7.87 | norisoprenoid group F-deoxyhexose-hexose-pentose ($C_{30}H_{50}O_{16}$) | 711.30718 666.30886 | 0.51 | | 503.25116 $[M-H-hexose-H_2O]^-$ 371.20758 $[M-H-pentose-hexose+H_2O]^-$ | $R^2 < 0.7$ |
| 169 | 3 | 4–5 | 7.91 | 4-vinylguaiacol-hexose-hexose[1] ($C_{21}H_{30}O_{12}$) | 473.16603 474.17330 | 0.26 | | 161.04425 $[Hexose-H-H_2O]^-$ | MP4: < DL MP5: < DL |
| 170 | 3 | 1, 4–5 | 8.02 | ipsdienol-deoxypentose-hexose ($C_{21}H_{34}O_9$) | 429.21262 430.21989 | 0.37 | | 267.15981 $[M-H-hexose+H_2O]^-$ 249.14843 $[M-H-hexose]^-$ 161.04522 $[Hexose-H-H_2O]^-$ | MP1: $R^2 < 0.7$ MP4: $R^2 < 0.7$ MP5: $R^2 < 0.7$ |
| 171 | 3 | 4 | 8.20 | hydroxycitronellol-pentose-hexose 2[6] ($C_{21}H_{40}O_{11}$) | 513.25459 468.25641 | 0.25 | | 467.24917 $[M-H]^-$ 335.20700 $[M-H-pentose-H + H_2O]^-$ 161.044860 $[Hexose-H + H_2O]^-$ | $R^2 < 0.7$ |
| 172 | 3 | 4 | 8.22 | hydroxycitronellol-hexose-deoxyhexose 3 ($C_{22}H_{42}O_{11}$) | 527.27010 482.27191 | 0.51 | | 481.26464 $[M-H]^-$ 365.21807 $[M + HCOOH-H-hexose+H_2O]^-$ 161.04515 $[Hexose-H-H_2O]^-$ | $R^2 < 0.7$ |
| 173 | 3 | 4 | 8.26 | monoterpenol-deoxypentose-deoxyhexose-hexose 3 ($C_{27}H_{46}O_{13}$) | 577.28543 578.29271 | 1.02 | | 161.04560 [Hexose-H]- | $R^2 < 0.7$ |
| 174 | 3 | 4 | 8.29 | geranic acid-hexose-pentose-pentose 2 ($C_{26}H_{42}O_{15}$) | 593.24470 594.25197 | 0.25 | | 179.05637 $[Hexose-H]^-$, 161.04576 $[Hexose-H-H_2O]^-$, 149.04472 $[Pentose-H]^-$ | $R^2 < 0.7$ |
| 175 | 3 | 4 | 8.42 | monoterpenol-deoxyhexose-hexose-pentose ($C_{27}H_{46}O_{14}$) | 593.28044 594.28772 | 0.83 | | 131.03474 $[Pentose-H-H_2O]^-$ | $R^2 < 0.7$ |
| 176 | 3 | 4 | 8.64 | citronellol/dihydromyrcenol-pentose-hexose[6,9] ($C_{21}H_{38}O_{10}$) | 449.23897 450.24625 | 0.66 | | 287.18528 $[M-H-hexose+H_2O]^-$ | $R^2 < 0.7$ |
| 177 | 3 | 4 | 8.72 | monoterpendiol-hexose-hexose 2[10] ($C_{22}H_{38}O_{12}$) | 493.22870 494.23598 | 0.40 | | 161.04507 $[Hexose-H-H_2O]^-$ | $R^2 < 0.7$ |
| 178 | 3 | 4 | 8.73 | citronellol/dihydromyrcenol-deoxyhexose-hexose-pentose 2 ($C_{27}H_{48}O_{14}$) | 595.29623 596.30351 | 0.60 | | 161.04546 $[Hexose-H-H_2O]^-$ | $R^2 < 0.7$ |
| 179 | 3 | 1 | 8.74 | ipsdienol-pentose-hexose 2 ($C_{21}H_{34}O_{10}$) | 445.20742 446.21470 | 0.10 | | 283.15365 $[M-H-hexose+H_2O]^-$ | $R^2 < 0.7$ |
| 180 | 3 | 2–3 | 8.88 | citronellol/dihydromyrcenol-pentose-pentose-pentose ($C_{25}H_{44}O_{13}$) | 551.26942 552.27670 | 1.72 | | 149.04472 $[Pentose-H]^-$ | MP 2: $R^2 < 0.7$ MP 3: $R^2 < 0.7$ |
| 181 | 3 | 5 | 8.85 | ipsdienol-pentose-hexose 3 ($C_{21}H_{34}O_{10}$) | 445.20789 446.21517 | 1.16 | | 283.15365 $[M-H-hexose+H_2O]^-$ | $R^2 < 0.7$ |
| 182 | 3 | 1, 4 | 9.11 | citronellol/dihydromyrcenol-hexose-deoxyhexose 2 ($C_{22}H_{40}O_{10}$) | 463.25452 464.26180 | 0.42 | | 301.20310 $[M-H-hexose+H_2O]^-$ | MP 1: $R^2 < 0.7$ MP 4: $R^2 < 0.7$ |
| 183 | 3 | 1, 4 | 9.18 | citronellol/dihydromyrcenol-hexose-deoxyhexose-deoxyhexose ($C_{28}H_{50}O_{14}$) | 609.31204 610.31932 | 0.32 | | 447.25894 $[M-H-hexose+H_2O]^-$ 429.25065 $[M-H-hexose]^-$ | MP 1: $R^2 < 0.7$ MP 4: $R^2 < 0.7$ |
| 184 | 3 | 1, 4–5 | 9.37 | geranic acid-hexose-deoxyhexose[6,10] ($C_{22}H_{36}O_{11}$) | 521.22362 476.22543 | 0.38 | 167.1081 | 475.21816 $[M-H]^-$ | MP1: $R^2 < 0.7$ MP4: $R^2 < 0.7$ MP5: $R^2 < 0.7$ |
| 185 | 3 | 1, 4 | 9.97 | monoterpenol-deoxypentose-deoxyhexose-hexose 4 ($C_{27}H_{46}O_{13}$) | 577.28631 578.29359 | 0.50 | | 161.04537 $[Hexose-H-H_2O]^-$ | MP 1: $R^2 < 0.7$ MP 4: $R^2 < 0.7$ |

< DL under detection limit. [a] Precursor category: (1) Fragments in the MS-MS spectrum are consistent with the precursor structure, and there is a significant correlation ($R^2 > 0.7$) between precursor content and the aroma released during hydrolysis; (2) The structure is supported by the fragments present in the MS-MS spectrum, but no

correlation can be established; (3) Fragments in the MS-MS spectrum are consistent with the precursor structure, but there is no significant correlation. [b] Mobile phase in which the precursor has been identified. [c] Retention time. [d] Experimentally measured mass/charge ratio. [e] Experimental molecular mass. [f] Mass error between the theoretical and experimental *m/z* values in parts per million. [g] Determination coefficient between the signals obtained in SPME-GC–MS and UHPLC-QTOF-MS. All correlations shown are statistically significant ($p < 0.05$).
Publications in which these types of precursors have been described:
[1](Barnaba, Larcher, et al., 2018). [2](Caffrey et al., 2019). [3](Caffrey et al., 2020). [4](Caffrey et al., 2022). [5](Cebrián-Tarancón et al., 2021). [6](Wei et al., 2021). [7](Gardiman et al., 2023). [8](Barnaba, Dellacassa, et al., 2018). [9](Flamini et al., 2014). [10](Ghaste et al., 2015). [11](Godshaw et al., 2019). [12](Barnaba et al., 2017). [13](Yang et al., 2025).

norisoprenoids are isomers with at least 9 different exact masses. Some of the masses could be related to several different aglycones and then are typically classified into 7 Groups marked with A to G letters (Caffrey et al., 2020), as can be seen in the Supplementary Material Table IX.

Among the identified precursors in Category 1, there are one disaccharide from Group A (no. 29, corresponding to a theoretical *m/z* for the deprotonated aglycone of 207.1290 - see theoretical deprotonated aglycone exact masses in Supplementary Material Table IX), two disaccharides from Group C (no. 24, 70, theoretical *m/z* 211.1703), five precursors from Group E (theoretical *m/z* 223.1339): three disaccharides (no. 12, 35 ≈ 67,) and two monosaccharides (no. 13 ≈ 30), six precursors from Group F (theoretical *m/z* 225.1495): including one monosaccharide (no. 17) and six disaccharides (no. 18 ≈ 22 ≈ 26, 31, 59), and four disaccharides of hydroxy-norisoprenoid group G (no. 11 ≈ 19, 41 ≈ 58, theoretical *m/z* 243.1596).

These precursors were primarily found in MP4-MP5, with some also present in MP1, MP2 and MP3, which is consistent with the distribution of aromas in the fractions (see Figs. 1 D, 1H, and 2 A-D, for *β*-ionone, *α*-ionone, *β*-damascenone, Riesling acetal, TDN, and vitispiranes, respectively). Unfortunately, the close polarities and molecular sizes of the different precursors make that precursors of norisoprenoids behave like a "pack" in which it is not possible differentiate which precursor is specifically linked to a specific aroma molecule.

Seven of the twelve different types of norisoprenoid precursors identified (no. 11 ≈ 19, 12, 13 ≈ 30, 17, 29, 41 ≈ 58, 59) had already been described during the analysis of grape glycosidic aroma precursors by UHPLC-QTOF-MS (Caffrey et al., 2020, 2022; Gardiman et al., 2023; Wei et al., 2021) or UHPLC-DAD (Cebrián-Tarancón et al., 2021).

*3.3.2.3. Potential volatile phenol precursors.* Two potential precursors of guaiacol (no. 1 and 2) and one potential precursor of 4-ethylguaiacol (no. 55) were identified, all of which showed a positive correlation with the concentration of guaiacol in the hydrolysed fractions analysed by SPME-GC–MS. These three precursors were found in MP4, where the highest concentration of guaiacol was observed in the SPME-GC–MS analysis. Precursors 1 and 2 have already been found by Barnaba, Larcher, et al. (2018) during the metabolomic profiling of food tannins sourced from commercial retailers and wineries.

### *3.3.3. Precursors with consistent MS-MS but unassessed aroma correlation (category 2)*

This category comprises the precursors of polar aroma compounds which were not the target analytes of the SPME-GC–MS method (furaneol, sinapaldehyde, coniferaldehyde), or that, although included (vanillin and related compounds, eugenol and isoeugenol and ethyl leucate), were not found in the hydrolysed fractions above the detection limit of the GC–MS method. This is a limitation of the GC method used. Because of the high number of fractions to analyse, and because of the limited volume available, a HS-SPME-GC–MS strategy was chosen, which is easily automated, minimizes sample preparation and can be very sensitive, but only for not very polar compounds. Polar volatile molecules are poorly detectable by head-space methods, and their sensitive determination requires liquid-liquid or liquid-solid extractions, which inevitably, mean using longer, more tedious and more expensive approaches, which could not be afforded in the present research. Because of this reason, for all those aroma molecules, some of them highly relevant to wine aroma, it was not possible to assess the correlation precursor/aroma formed and the identification of the precursors was, therefore, based solely on the fragments in the mass-mass spectra that justified the proposed structure.

42 precursors in this category were identified, including precursors of volatile phenols, compounds from the vanillin family, ethyl leucate, and others.

*3.3.3.1. Potential volatile phenol precursors.* Nine precursors of volatile phenols were identified, of six different types: two disaccharides (no. 109, 113) and four trisaccharides (no. 110 ≈ 112 ≈ 116) corresponding to eugenol or its isomer, isoeugenol; and four precursors of ethoxymethylmethoxyphenol: one monosaccharide (no. 105) and three trisaccharides (no. 80 ≈ 89, 114). As far as we know, only ethoxymethylmethoxyphenol-hexose (no. 105), eugenol-hexose-deoxyhexose (no. 109) and eugenol-pentose-hexose (no. 113) have been previously reported in winemaking grapes (Barnaba et al., 2017; Barnaba, Dellacassa, et al., 2018; Barnaba, Larcher, et al., 2018; Yang et al., 2025). It should be noted that, as can be seen in Table 1, the three precursors were present in mobile phases 1, 4–5, in which also elute the precursors of the other phenols analysed (4-vinylphenol, 4-vinylguaicol, 4-ethylphenol, syringol and guaiacol, peaks around MP 1–2, 4–5; Figs. 1 E-G and 2H—I), which is consistent with the proposed structures.

*3.3.3.2. Potential precursors of the vanillin family.* Nineteen precursors of the polar aroma compounds vanillin (logP 1.39), acetovanillone (logP 1.19), and syringaldehyde (logP 0.86) were identified, belonging to eight different types. These include four precursors of acetovanillone: three monosaccharides (no. 76 ≈ 79 ≈ 90) and one disaccharide (no. 83); nine precursors of vanillin: five monosaccharides (no. 81 ≈ 88 ≈ 93 ≈ 106, 98) and four disaccharides (no. 84 ≈ 95 ≈ 103, 94); and six precursors of syringaldehyde: four monosaccharides (no. 85 ≈ 92 ≈ 97 ≈ 107) and two disaccharides (no. 82 ≈ 86).

All of these precursors have been previously reported in the glycosidic profiling of monovarietal wines or grape varieties such as Cabernet Cantor, Prior, Chardonnay, Merlot and Glera (Barnaba et al., 2017; Barnaba, Dellacassa, et al., 2018; Barnaba, Larcher, et al., 2018; Gardiman et al., 2023), except for acetovanillone-hexose-hexose (no. 83).

*3.3.3.3. Potential precursors of ethyl leucate.* Six precursors of ethyl leucate from three different types were identified: four trisaccharides (no. 96 ≈ 102 ≈ 104 ≈ 108), one monosaccharide (no. 100), and one disaccharide (no. 117). It has been observed that this ester is progressively released from its precursors during wine aging (Denat et al., 2022). To the best of our knowledge, these precursors have not been reported before.

*3.3.3.4. Other precursors.* In this category, four precursors of furaneol were identified: three disaccharides (no. 77, 87, 91) and one trisaccharide (no. 78). Furaneol is commonly found in wines (Bueno et al., 2023; de-la-Fuente-Blanco & Ferreira, 2020; Ferreira et al., 2002), and its formation results from glycosidic precursors, since chemical degradation of sugars via the Maillard reaction cannot occur under such conditions. However, only a few furaneol glycoside structures such as furaneol-pentose-hexose (no. 77) have been identified in grapes (Wei et al., 2021). The remaining furaneol precursors described in this study have not been previously reported.

In addition, one precursor of coniferaldehyde (dissacharide, no. 99);

and three precursors of sinapaldehyde were identified: one dissacharide (no. 101) and two monosaccharides (no. 111 ≈ 115). Coniferaldehyde and sinapaldehyde are phenolic aldehydes derived from lignin biosynthesis in plants (Fotakis et al., 2024), and as far as we know, these precursors have not been described previously.

It is worth noting that this study also enabled the identification of a large number of polyphenols — including stilbenes, benzoic acid derivatives, and flavonoids — as well as various alcohols. Since these compounds are not among the aromatic compounds of interest in this study, as they are not varietal aromas, no further discussion will be made regarding them.

#### 3.3.4. *Precursors with consistent MS-MS but no significant aroma correlation (category 3)*

This category includes precursors of aroma molecules well detected by the HS-SPME-GC–MS method, for which their MS-MS spectra contain fragments that support their chemical structures but for which there is no significant correlation between the precursor signal and the concentration of the aroma found in the hydrolysed fractions. Therefore, they are not expected to be major precursors. Following these criteria, 68 precursors were identified in this category, including precursors of terpenes, norisoprenoids, volatile phenols, and derivatives of cinnamic acid.

*3.3.4.1. Potential terpene precursors.* Twenty-nine terpene precursors were identified, belonging to 23 different types, 13 of which were distinct from those in Category 1. Among these terpene precursors are: six precursors of ipsdienol: two trisaccharides (no. 129, 156) and four disaccharides (no. 165 ≈ 179 ≈ 181, 170); three trisaccharides of monoterpenol (no. 173 ≈ 185, 175), seven precursors of monoterpendiol: two of them trisaccharides (no. 134 ≈ 155) and five disaccharides (no. 158, 159 ≈ 162 ≈ 166, 177), one trisaccharide of dihydromonoterpentriol (no. 128), one monosaccharide of dehydromonoterpentriol (no. 164) and one disaccharide of dihydromonoterpentetraol (no. 148).

Additionally, five precursors of citronellol or its isomer dihydromyrcenol were identified: three trisaccharides (no. 178, 180, 183) and two disaccharides (no. 176, 182), three precursors of hydroxycitronellol (no. 167, 171, 172) and two precursors of geranic acid (no. 174, 184).

Just like the terpene precursors in Category 1, most of the terpene precursors identified in Category 3 were found around MP4–5, which agrees with the peaks observed in Figs. 4 B and 7 E-G.

Among the twenty-three different types of terpene precursors only six (no. 159 ≈ 162 ≈ 166, 164, 171, 176, 177, 184) have been found during the analysis of glycosidic aroma precursors in winemaking grapes (Barnaba, Dellacassa, et al., 2018; Caffrey et al., 2020, 2022; Cebrián-Tarancón et al., 2021, 2021; Flamini et al., 2014; Gardiman et al., 2023; Ghaste et al., 2015; Wei et al., 2021).

*3.3.4.2. Potential precursors of norisoprenoids.* Three norisoprenoids of Group F (no. 140, 153, 168) were identified, one of them (no. 168) represents a type not described in Category 1. The Group F precursors were found in MP 4–5, which coincides with the location of the Riesling acetal in the hydrolysed fractions (Fig. 2 B). Of these, only norisoprenoid Group F-hexose-hexose (no. 140) has been previously reported by Caffrey et al. (2020) in their analysis of glycosides by UHPLC-QTOF-MS in Riesling and Muscat of Alexandria berries.

*3.3.4.3. Potential precursors of volatile phenols.* Eighteen volatile phenols belonging to fourteen distinct types were identified. Among them, eight are precursors of syringol: two of them are monosaccharides (no. 118, 143) and six are disaccharides (no. 120 ≈ 130, 127 ≈ 133 ≈ 161 ≈ 163). Three 4-ethylphenol precursors were also identified: one disaccharide (no. 135), one monosaccharide (no.138) and one trisaccharide (no. 160). Additionally, five precursors of cresol were identified: three disaccharides (no. 142, 152 and 157) and two trisaccharides (no. 144 and 154), as well as one disaccharide of 4-vinylguaiacol (no. 169) and one trisaccharide of 4-ethylguaiacol (no. 137). Most of these precursors were found in MP4–5, where peaks corresponding to 4-ethylphenol and syringol were identified in the SPME-GC–MS analysis (Fig. 1 G and 2H, respectively). The concentration of *m*-cresol was found to be below the detection limit in all fractions, whereas o-cresol was detected exclusively in MP 1–2 at concentrations close to the detection limit (graph not included). Their precursors, in fact, were present in MP 4–5.

4-vinylguaiacol was found in the SPME-GC–MS analysis in the early mobile phases (Fig. 4A); however, the identified precursor was found in MP 4–5, where its concentration was below the detection limit.

Several of these precursors (no. 118, 120, 127, 130, 133, 135, 138, 144, 152, 157, 161, 163, 169) have been previously found during the analysis of glycosidic aroma precursors in several *Vitis vinifera* varieties such as Muscat of Alexandria, Riesling, Sauvignon Blanc, Gewürztraminer, Glera and Chardonnay (Barnaba, Dellacassa, et al., 2018; Barnaba et al., 2017; Barnaba, Larcher, et al., 2018; Caffrey et al., 2019, 2020, 2022; Cebrián-Tarancón et al., 2021; Gardiman et al., 2023; Ghaste et al., 2015; Wei et al., 2021; Yang et al., 2025).

*3.3.4.4. Potential precursors of ethyl cinnamate and dihydrocinnamate.* Although little is known about the precursors of ethyl cinnamate and dihydrocinnamate, it is likely that they are produced through the esterification of the corresponding acids. Due to the presence of a hydroxyl group, these acids can react with sugars to form glycosidic bonds. For this reason, this type of precursor was included in the Target List. Eighteen cinnamate and dihydrocinnamate precursors belonging to seven distinct types were identified. These included five monohydroxymethoxycinnamic acid precursors (no. 121 ≈ 147, 122, 131 ≈ 149), five monohydroxycinnamic acid precursors (no. 119 ≈ 125, 124 ≈ 146 ≈ 150), and eight dihydroxycinnamic acid precursors (no. 123 ≈ 126 ≈ 132 ≈ 139 ≈ 145 ≈ 151, 136 ≈ 141). These precursors have been all previously reported in grapes (Barnaba et al., 2017; Barnaba, Dellacassa, et al., 2018; Barnaba, Larcher, et al., 2018).

Cinnamate and ethyl dihydrocinnamate were detected above their SPME-GC–MS detection limit in only four different fractions (three for cinnamate and one for dihydrocinnamate). However, these compounds were likely present at lower concentrations in adjacent fractions, remaining below their detection limit. This, combined with the high sensitivity of UHPLC-QTOF-MS, which can detect very low concentrations of analytes, may explain the discrepancies between the signals obtained by SPME-GC–MS and UHPLC-QTOF-MS, which prevent significant correlations for these compounds. For this reason, all ethyl cinnamate and dihydrocinnamate precursors are categorised as Category 3 and do not appear in Category 1.

## 4. Conclusions

Size exclusion chromatography using Toyopearl has demonstrated that the aroma precursors in grapes are low-molecular-mass compounds. Silica-gel fractionation has revealed that the precursors had quite different polarities; 92 out of 96 of the fractions developed an aroma. Targeted quantifiable aroma compounds (6 terpenols, 6 norisoprenoids, 5 phenols and 2 cinnamic esters) eluted in 55 fractions of, roughly, three different polarities (very low, low and intermediate). Polar or ultra-trace aroma compounds, such as vanillin derivatives, furaneol and ethyl leucate derivatives, could not be quantified, although potential precursors for these compounds were tentatively identified.

The systematic combination of C18, size-exclusion using Toyopearl and silica-gel fractionation, together with complementary analytical techniques (targeted GC–MS and untargeted UHPLC-MS), proved to be an effective approach for isolating and identifying a broad spectrum of glycosidic aroma precursors. A total of 185 glycosidic precursors were

identified at three different confidence levels attending to the verification of up to three identity criteria (exact mass, MS/MS fragmentation consistent with the proposed structure and significant correlation with the aroma molecule). The precursors identified included 83 terpenes, 30 volatile phenols, 22 cinnamic acid derivative, 21 norisoprenoid, 19 vanillin derivatives, 6 ethyl leucate derivatives and 4 furaneol precursors compounds. Of these, 98 had not been previously described.

Further studies should employ GC quantitative methods more sensitive to polar aroma compounds, such as vanillin derivatives and furaneol. They should also incorporate additional identification criteria such as ion mobility to enhance and refine the databases of aroma precursors.

## CRediT authorship contribution statement

**Belén González-Martínez:** Writing – review & editing, Writing – original draft, Methodology, Investigation, Formal analysis. **Elayma Sánchez-Acevedo:** Writing – original draft, Methodology, Investigation, Formal analysis. **Arancha de-la-Fuente-Blanco:** Writing – review & editing, Writing – original draft, Methodology, Investigation, Formal analysis. **Ignacio Ontañón:** Writing – original draft, Methodology, Investigation, Formal analysis. **Ricardo Lopez:** Writing – review & editing, Methodology, Investigation, Conceptualization. **Vicente Ferreira:** Writing – review & editing, Project administration, Funding acquisition, Conceptualization.

## Funding sources

The authors would like to thank Dr. Marivel González and Dr. María Pilar Sáenz for conducting the fractionation on Toyopearl. B.G.M acknowledges the Department of Science, University and Knowledge Society from DGA her predoctoral grant (2024 call). E.S.A has received a grant (PRE2018–084968) from the Spanish FPI programs. LAAE acknowledges the continuous support of Gobierno de Aragón (T29) and European Social Fund. Funded by the Spanish Ministry of Science, Innovation and Universities and the European Union (project PID2021-126031OB-C21).

## Declaration of competing interest

The authors declare the following financial interests/personal relationships which may be considered as potential competing interests: Vicente Ferreira reports financial support was provided by Spanish Ministry of Science, Innovation and Universities. Belen Gonzalez-Martinez reports financial support was provided by Government of Aragon Department of Science Technology and University. Elayma Sanchez-Acevedo reports financial support was provided by Spanish Ministry of Science, Innovation and Universities. If there are other authors, they declare that they have no known competing financial interests or personal relationships that could have appeared to influence the work reported in this paper.

## Appendix A. Supplementary data

Supplementary data to this article can be found online at https://doi.org/10.1016/j.foodchem.2025.147361.

## Data availability

Data used for the research are described in the article.

## References

Alegre, Y., Arias-Pérez, I., Hernández-Orte, P., & Ferreira, V. (2020). Development of a new strategy for studying the aroma potential of winemaking grapes through the accelerated hydrolysis of phenolic and aromatic fractions (PAFs). *Food Research International, 127*, Article 108728. https://doi.org/10.1016/j.foodres.2019.108728

Arapitsas, P., Corte, A. D., Gika, H., Narduzzi, L., Mattivi, F., & Theodoridis, G. (2016). Studying the effect of storage conditions on the metabolite content of red wine using HILIC LC–MS based metabolomics. *Food Chemistry, 197*, 1331–1340. https://doi.org/10.1016/j.foodchem.2015.09.084

Barnaba, C., Dellacassa, E., Nicolini, G., Giacomelli, M., Roman Villegas, T., Nardin, T., & Larcher, R. (2017). Targeted and untargeted high resolution mass approach for a putative profiling of glycosylated simple phenols in hybrid grapes. *Food Research International, 98*, 20–33. https://doi.org/10.1016/j.foodres.2017.01.011

Barnaba, C., Dellacassa, E., Nicolini, G., Nardin, T., Serra, M., & Larcher, R. (2018). Non-targeted glycosidic profiling of international wines using neutral loss-high resolution mass spectrometry. *Journal of Chromatography A, 1557*, 75–89. https://doi.org/10.1016/j.chroma.2018.05.008

Barnaba, C., Larcher, R., Nardin, T., Dellacassa, E., & Nicolini, G. (2018). Glycosylated simple phenolic profiling of food tannins using high resolution mass spectrometry (Q-Orbitrap). *Food Chemistry, 267*, 196–203. https://doi.org/10.1016/j.foodchem.2017.11.048

Baumes, R. (2009). Wine aroma precursors. In M. V. Moreno-Arribas, & M. C. Polo (Eds.), *Wine chemistry and biochemistry* (pp. 251–274). Springer. https://doi.org/10.1007/978-0-387-74118-5_14.

Bueno, M., Zapata, J., Culleré, L., Franco-Luesma, E., De-La-Fuente-Blanco, A., & Ferreira, V. (2023). Optimization and validation of a method to determine enolones and vanillin derivatives in wines—Occurrence in spanish red wines and mistelles. *Molecules, 28*(10), 4228. https://doi.org/10.3390/molecules28104228

Burney, J., Kennel, C. F., & Victor, D. G. (2013). Getting serious about the new realities of global climate change. *Bulletin of the Atomic Scientists, 69*(4), 49–57. https://doi.org/10.1177/0096340213493882

Caffrey, A., Lafontaine, S., Dailey, J., Varnum, S., Lerno, L. A., Zweigenbaum, J., … Ebeler, S. E. (2022). Characterization of *Humulus lupulus* glycosides with porous graphitic carbon and sequential high performance liquid chromatography quadrupole time-of-flight mass spectrometry and high performance liquid chromatography fractionation. *Journal of Chromatography A, 1674*, Article 463130. https://doi.org/10.1016/j.chroma.2022.463130

Caffrey, A., Lerno, L., Rumbaugh, A., Girardello, R., Zweigenbaum, J., Oberholster, A., & Ebeler, S. E. (2019). Changes in smoke-taint volatile-phenol glycosides in wildfire smoke-exposed Cabernet Sauvignon grapes throughout winemaking. *American Journal of Enology and Viticulture, 70*(4), 373–381. https://doi.org/10.5344/ajev.2019.19001

Caffrey, A., Lerno, L., Zweigenbaum, J., & Ebeler, S. E. (2020). Direct analysis of glycosidic aroma precursors containing multiple aglycone classes in *Vitis vinifera* berries. *Journal of Agricultural and Food Chemistry, 68*(12), 3817–3833. https://doi.org/10.1021/acs.jafc.9b08323

Cebrián-Tarancón, C., Oliva, J., Cámara, M.Á., Alonso, G. L., & Salinas, M. R. (2021). Analysis of intact glycosidic aroma precursors in grapes by high-performance liquid chromatography with a diode array detector. *Foods, 10*(1), 191. https://doi.org/10.3390/foods10010191

Cordente, A. G., Capone, D. L., & Curtin, C. D. (2015). Unravelling glutathione conjugate catabolism in *Saccharomyces cerevisiae*: The role of glutathione/dipeptide transporters and vacuolar function in the release of volatile sulfur compounds 3-mercaptohexan-1-ol and 4-mercapto-4-methylpentan-2-one. *Applied Microbiology and Biotechnology, 99*(22), 9709–9722. https://doi.org/10.1007/s00253-015-6833-5

D'Ambrosio, M., Harghel, P., & Guantieri, V. (2013). Isolation of intact glycosidic aroma precursors from grape juice by hydrophilic interaction liquid chromatography. *Australian Journal of Grape and Wine Research, 19*(2), 189–192. https://doi.org/10.1111/ajgw.12028

de-la-Fuente-Blanco, A., & Ferreira, V. (2020). Gas chromatography olfactometry (GC-O) for the (semi)quantitative screening of wine aroma. *Foods, 9*(12), Article 12. https://doi.org/10.3390/foods9121892

Denat, M., Ontañón, I., Querol, A., & Ferreira, V. (2022). The diverse effects of yeast on the aroma of non-sulfite added white wines throughout aging. *LWT, 158*, Article 113111. https://doi.org/10.1016/j.lwt.2022.113111

Ferreira, V., Herrero, P., Zapata, J., & Escudero, A. (2015). Coping with matrix effects in headspace solid phase microextraction gas chromatography using multivariate calibration strategies. *Journal of Chromatography A, 1407*, 30–41. https://doi.org/10.1016/j.chroma.2015.06.058

Ferreira, V., & López, R. (2019). The actual and potential aroma of winemaking grapes. *Biomolecules, 9*(12), 818. https://doi.org/10.3390/biom9120818

Ferreira, V., Ortín, N., Escudero, A., López, R., & Cacho, J. (2002). Chemical characterization of the aroma of grenache rosé wines: Aroma extract dilution analysis, quantitative determination, and sensory reconstitution studies. *Journal of Agricultural and Food Chemistry, 50*(14), 4048–4054. https://doi.org/10.1021/jf0115645

Flamini, R., De Rosso, M., Panighel, A., Dalla Vedova, A., De Marchi, F., & Bavaresco, L. (2014). Profiling of grape monoterpene glycosides (aroma precursors) by ultra-high performance-liquid chromatography-high resolution mass spectrometry (UHPLC/QTOF). *Journal of Mass Spectrometry, 49*(12), 1214–1222. https://doi.org/10.1002/jms.3441

Fotakis, C., Andreou, V., Christodouleas, D. C., & Zervou, M. (2024). The metabolic and antioxidant activity profiles of aged greek grape marc spirits. *Foods, 13*(11), Article 11. https://doi.org/10.3390/foods13111664

Gardiman, M., De Rosso, M., De Marchi, F., & Flamini, R. (2023). Metabolomic profiling of different clones of vitis vinifera L. cv. 'Glera' and 'Glera lunga' grapes by high-resolution mass spectrometry. *Metabolomics: Official Journal of the Metabolomic Society, 19*(4), 25. https://doi.org/10.1007/s11306-023-01997-w

Ghaste, M., Narduzzi, L., Carlin, S., Vrhovsek, U., Shulaev, V., & Mattivi, F. (2015). Chemical composition of volatile aroma metabolites and their glycosylated

precursors that can uniquely differentiate individual grape cultivars. *Food Chemistry, 188*, 309–319. https://doi.org/10.1016/j.foodchem.2015.04.056

Godshaw, J., Hjelmeland, A. K., Zweigenbaum, J., & Ebeler, S. E. (2019). Changes in glycosylation patterns of monoterpenes during grape berry maturation in six cultivars of *Vitis vinifera*. *Food Chemistry, 297*, Article 124921. https://doi.org/10.1016/j.foodchem.2019.05.195

Gunata, Y. Z., Bayonove, C. L., Baumes, R. L., & Cordonnier, R. E. (1985). The aroma of grapes I. Extraction and determination of free and glycosidically bound fractions of some grape aroma components. *Journal of Chromatography A, 331*, 83–90. https://doi.org/10.1016/0021-9673(85)80009-1

Gunata, Y. Z., Bayonove, C. L., Tapiero, C., & Cordonnier, R. E. (1990). Hydrolysis of grape monoterpenyl *β*-D-glucosides by various *β*-glucosidases. *Journal of Agricultural and Food Chemistry, 38*(5), 1232–1236. https://doi.org/10.1021/jf00095a016

Hampel, D., Robinson, A. L., Johnson, A. J., & Ebeler, S. E. (2014). Direct hydrolysis and analysis of glycosidically bound aroma compounds in grapes and wines: Comparison of hydrolysis conditions and sample preparation methods. *Australian Journal of Grape and Wine Research, 20*(3), 361–377. https://doi.org/10.1111/ajgw.12087

Hjelmeland, A. K., & Ebeler, S. E. (2015). Glycosidically bound volatile aroma compounds in grapes and wine: A review. *American Journal of Enology and Viticulture, 66*, 1–11. https://doi.org/10.5344/ajev.2014.14104

Hjelmeland, A. K., Zweigenbaum, J., & Ebeler, S. E. (2015). Profiling monoterpenol glycoconjugation in *Vitis vinifera* L. cv. Muscat of Alexandria using a novel putative compound database approach, high resolution mass spectrometry and collision induced dissociation fragmentation analysis. *Analytica Chimica Acta, 887*, 138–147. https://doi.org/10.1016/j.aca.2015.06.026

Liu, J., Zhu, X.-L., Ullah, N., & Tao, Y.-S. (2017). Aroma glycosides in grapes and wine. *Journal of Food Science, 82*(2), 248–259. https://doi.org/10.1111/1750-3841.13598

Loscos, N., Hernández-Orte, P., Cacho, J., & Ferreira, V. (2009). Comparison of the suitability of different hydrolytic strategies to predict aroma potential of different grape varieties. *Journal of Agricultural and Food Chemistry, 57*(6), 2468–2480. https://doi.org/10.1021/jf803256e

Mateo, J. J., & Jiménez, M. (2000). Monoterpenes in grape juice and wines. *Journal of Chromatography A, 881*(1), 557–567. https://doi.org/10.1016/S0021-9673(99)01342-4

Parker, M., Capone, D. L., Francis, I. L., & Herderich, M. J. (2018). Aroma precursors in grapes and wine: Flavor release during wine production and consumption. *Journal of Agricultural and Food Chemistry, 66*(10), 2281–2286. https://doi.org/10.1021/acs.jafc.6b05255

Parr, W. V., Heatherbell, D., & White, K. G. (2002). Demystifying wine expertise: Olfactory threshold, perceptual skill and semantic memory in expert and novice wine judges. *Chemical Senses, 27*(8), 747–755. https://doi.org/10.1093/chemse/27.8.747

Petropoulos, S., Kanellopoulou, A., Paraskevopoulos, I., Kotseridis, Y., & Kallithraka, S. (2017). Characterization of grape and wine proanthocyanidins of Agiorgitiko (*Vitis vinifera L.* cv.) cultivar grown in different regions of Nemea. *Journal of Food Composition and Analysis, 63*, 98–110. https://doi.org/10.1016/j.jfca.2017.07.038

Resco, P., Iglesias, A., Bardají, I., & Sotés, V. (2016). Exploring adaptation choices for grapevine regions in Spain. *Regional Environmental Change, 16*(4), 979–993. https://doi.org/10.1007/s10113-015-0811-4

Sáenz-Navajas, M.-P., Avizcuri, J.-M., Ferrero-del-Teso, S., Valentin, D., Ferreira, V., & Fernández-Zurbano, P. (2017). Chemo-sensory characterization of fractions driving different mouthfeel properties in red wines. *Food Research International, 94*, 54–64. https://doi.org/10.1016/j.foodres.2017.02.002

Salinas, M. R., de la Hoz, K. S., Zalacain, A., Lara, J. F., & Garde-Cerdán, T. (2012). Analysis of red grape glycosidic aroma precursors by glycosyl glucose quantification. *Talanta, 89*, 396–400. https://doi.org/10.1016/j.talanta.2011.12.050

San-Juan, F., Cacho, J., Ferreira, V., & Escudero, A. (2012). Aroma chemical composition of red wines from different price categories and its relationship to quality. *Journal of Agricultural and Food Chemistry, 60*(20), 5045–5056. https://doi.org/10.1021/jf2050685

Sarry, J.-E., & Günata, Z. (2004). Plant and microbial glycoside hydrolases: Volatile release from glycosidic aroma precursors. *Food Chemistry, 87*(4), 509–521. https://doi.org/10.1016/j.foodchem.2004.01.003

Schievano, E., D'Ambrosio, M., Mazzaretto, I., Ferrarini, R., Magno, F., Mammi, S., & Favaro, G. (2013). Identification of wine aroma precursors in *Moscato Giallo* grape juice: A nuclear magnetic resonance and liquid chromatography–mass spectrometry tandem study. *Talanta, 116*, 841–851. https://doi.org/10.1016/j.talanta.2013.07.049

Skouroumounis, G. K., & Sefton, M. A. (2000). Acid-catalyzed hydrolysis of alcohols and their *β*-D-glucopyranosides. *Journal of Agricultural and Food Chemistry, 48*(6), 2033–2039. https://doi.org/10.1021/jf9904970

Subileau, M., Schneider, R., Salmon, J.-M., & Degryse, E. (2008a). New insights on 3-mercaptohexanol (3MH) biogenesis in sauvignon blanc wines: Cys-3MH and (E)-hexen-2-al are not the major precursors. *Journal of Agricultural and Food Chemistry, 56*(19), 9230–9235. https://doi.org/10.1021/jf801626f

Subileau, M., Schneider, R., Salmon, J.-M., & Degryse, E. (2008b). Nitrogen catabolite repression modulates the production of aromatic thiols characteristic of sauvignon blanc at the level of precursor transport. *FEMS Yeast Research, 8*(5), 771–780. https://doi.org/10.1111/j.1567-1364.2008.00400.x

Wang, Y., Li, H.-Q., Gao, X.-T., Lu, H.-C., Peng, W.-T., Chen, W., … Wang, J. (2020). Influence of attenuated reflected solar radiation from the vineyard floor on volatile compounds in Cabernet Sauvignon grapes and wines of the north foot of Mt. Tianshan. *Food Research International, 137*, Article 109688. https://doi.org/10.1016/j.foodres.2020.109688

Wei, Y., Chen, Z., Zhang, X.-K., Duan, C.-Q., & Pan, Q.-H. (2021). Comparative analysis of glycosidic aroma compound profiling in three *Vitis vinifera* varieties by using ultra-high-performance liquid chromatography quadrupole-time-of-flight mass spectrometry. *Frontiers in Plant Science, 12*. https://doi.org/10.3389/fpls.2021.694979

Yang, W., Zheng, Z., Yang, Y., You, Y., Ye, D., Zhang, Z., Yu, K., Shi, Y., Duan, C., & Lan, Y. (2025). Identification of key precursors of eugenol and Syringol in wines using a Pseudo-targeted Metabolomic approach. *Food Chemistry, 477*, Article 143552. https://doi.org/10.1016/j.foodchem.2025.143552